Fall 1966

Heat transfer between a turbulent round jet and a segmented flat plate perpendicular to it

John Edward Chamberlain
New Jersey Institute of Technology

Copyright Warning & Restrictions

The copyright law of the United States (Title 17, United States Code) governs the making of photocopies or other reproductions of copyrighted material.

Under certain conditions specified in the law, libraries and archives are authorized to furnish a photocopy or other reproduction. One of these specified conditions is that the photocopy or reproduction is not to be "used for any purpose other than private study, scholarship, or research." If a, user makes a request for, or later uses, a photocopy or reproduction for purposes in excess of "fair use" that user may be liable for copyright infringement,

This institution reserves the right to refuse to accept a copying order if, in its judgment, fulfillment of the order would involve violation of copyright law.

Please Note: The author retains the copyright while the New Jersey Institute of Technology reserves the right to distribute this thesis or dissertation

Printing note: If you do not wish to print this page, then select "Pages from: first page # to: last page #" on the print dialog screen

HEAT TRANSFER BETWEEN A TURBULENT ROUND JET AND A SEGMENTED FLAT PLATE PERPENDICULAR TO IT.

BY

JOHN E. CHAMBERLAIN

A THESIS

PRESENTED IN PARTIAL FULFILLMENT OF

THE REQUIREMENTS FOR THE DEGREE

OF

MASTER OF SCIENCE IN MECHANICAL ENGINEERING

AT

NEWARK COLLEGE OF ENGINEERING

Newark, New Jersey
1966

ABSTRACT

Heat transfer between a room temperature, turbulent round jet and a segmented flat plate perpendicular to it has been investigated.

The heat transfer surface consisted of invar rings insulated from each other with silicone rubber. The source of heat was steam at atmospheric pressure condensing on the back of the heat transfer surface.

Since data were taken over a wide range of vertical distances between the nozzle and the flat surface both the potential cone and the fully developed regions of the jet were observed interacting with the heated plate.

It was determined that two modes of heat transfer occur; one in the potential cone region and the other in the fully developed region of the jet striking the plate. Results were successfully correlated at the stagnation point for all vertical distances between the jet and the plate. The decrease in heat transfer coefficient with increasing radial distance from the stagnation point has been successfully correlated in both the potential cone and the fully developed regions of the jet as well.

APPROVAL OF THESIS

HEAT TRANSFER BETWEEN A TURBULENT ROUND JET
AND A SEGMENTED FLAT PLATE PERPENDICULAR TO IT.

BY

JOHN EDWARD CHAMBERLAIN

FOR

DEPARTMENT OF MECHANICAL ENGINEERING

NEWARK COLLEGE OF ENGINEERING

BY

FACULTY COMMITTEE

APPROVED: _____

_____

_____

NEWARK, NEW JERSEY

JANUARY, 1967

ACKNOWLEDGEMENTS

An undertaking of this magnitude would not have been possible without the fellowship which was awarded to me by the Linde Division of the Union Carbide Corporation.

I also wish to thank my associates in the Mechanical Engineering Department who have given me assistance throughout the preparation of this thesis. In particular, Dr. Peter Hrycak, my thesis advisor, provided me with helpful suggestions and guidance throughout this work. Prof. Robert M. Jacobs gave me much assistance in designing the instrumentation. Mr. Walter Schmiedeskamp, the director of the machine shop, provided many useful suggestions related to the fabrication of the experimental apparatus. Mr. Frank Close assisted me in constructing the apparatus.

Typing and checking have been ably carried out by Mrs Diane DiNorcia and by my wife, Pat.

TABLE OF CONTENTS

	PAGE
INTRODUCTION	1
REVIEW OF PREVIOUS WORK	4
THE APPARATUS	11
THE TEST PROCEDURE	13
ANALYSIS OF RESULTS - GENERAL	16
ANALYSIS OF RESULTS - STAGNATION POINT HEAT TRANSFER	19
ANALYSIS OF RESULTS - RADIAL VARIATION OF LOCAL HEAT TRANSFER COEFFICIENTS	29
SUMMARY OF RESULTS	31
APPENDIX	33
REFERENCES	79

LIST OF FIGURES

FIGURE	TITLE	PAGE
1	Generalized Heat Transfer Variation at the Stagnation Point.	34
2	Radial Variation of Heat Transfer Coefficients.	34
3	The Air Supply and Flow Metering System	35
4	Heated Flat Plate Assembly	36
5	Detail View of the Heat Transfer Surface	37
6	Thermocouple Circuit Diagram	38
7	Photographs of the Test Apparatus	39
8	Photographs of the Test Apparatus	40
9	Effect of the Reynolds Number on Heat Transfer at the Stagnation Point	41
10	"Correlation of Heat Transfer Coefficients at the Stagnation Point of a Two-Dimensional Air Jet".	42
11(A)	Nusselt Number at the Stagnation Point vs. Reynolds Number Based on Air Properties at the Nozzle Exit.	43
11(B)	Nusselt Number at the Stagnation Point vs. Reynolds Number Based on Air Properties at the Nozzle Exit.	44
11(C)	Nusselt Number at the Stagnation Point vs. Reynolds Number Based on Air Properties at the Nozzle Exit.	45
11(D)	Log of $Nu/Pr^{0.33}$ at the Stagnation Point vs. Log of Reynolds Number Based on Air Properties at the Nozzle Exit	46
12	Velocity and Turbulence Decay Factor	47
13	Correlation of Stagnation Point Heat Transfer for $Z_n/D > 7$.	48
14	Overlay of Stagnation Point Heat Transfer Correlation Curves for the Potential Cone Region and the Fully Developed Flow Region.	49

FIGURE	TITLE	PAGE
15	Illustration of the Two Modes of Heat Transfer to an Impinging Round Jet.	50
16	Correlation of Radial Variation of Heat Transfer Coefficients with Fully Developed Jet Impinging on the Flat Plate.	51
17	Correlation of Radial Variation of Local Heat Transfer Coefficients in the Potential Cone for Re = 6700.	52
18	Correlation of Radial Variation of Local Heat Transfer Coefficients in the Potential Cone for Re = 13,900.	53
19	Correlation of Radial Variation of Local Heat Transfer Coefficients in the Potential Cone for Re = 26,000.	54
20	Correlation of Radial Variation of Local Heat Transfer Coefficients in the Potential Cone for Re = 54,000.	55
21	Correlation of Radial Variation of Local Heat Transfer Coefficients in the Potential Cone for Re = 67,500	56
22	Correlation of Radial Variation of Heat Transfer Coefficients with Potential Cone of Jet Impinging on Plate.	57

LIST OF TABLES

PAGE

ORIGINAL DATA 63ff.

NOMENCLATURE

Z_n - Vertical distance between nozzle and plate

D - Nozzle diameter

B - Slot width for two dimensional nozzle

x - Radial distance from the stagnation point

h - Local heat transfer coefficient at any point on the heat transfer surface

h_o - Heat transfer coefficient at the stagnation point

Re - Reynolds No. based on air properties at the nozzle exit. The characteristic length is D throughout this work except where otherwise noted.

Nu_o - Nusselt No. at the stagnation point. Characteristic lenght is D

Nu - Nusselt number at any point on the heat transfer surface other than the stagnation point.

Pr - Prandtl Number

q - Heat transfer per unit area per unit time ($B/ft^2/hr$)

k - Conductivity of invar (B/hr ft. °f)

L_i - Distance between thermocouples

T_i - Temperature drop across the invar ring

T_s - Surface temperature on the invar ring

T_j - Jet stagnation temperature

T_{ci} - Temperature at copper-invar interface

L_s - Total thickness of invar rings

F - Velocity and turbulence decay factor

Re_a - Reynolds Number of fluid jet as it arrives at the flat plate

INTRODUCTION

The use of round jets for the cooling of surfaces placed perpendicular to the axis of flow has numerous applications in industry. Single jets may be used for spot cooling or arrays of jets may be used to cool entire surfaces. The chief advantage of jet cooling is that for a given flow of fluid much higher local coefficients of heat transfer may be obtained than for the more conventional methods of convection heat transfer, due to the scouring action of the fluid near the heat transfer surface.

Some typical applications of jet cooling are as follows: The front face of the lance used to inject oxygen into a Basic Oxygen Process Steel Furnace is cooled by a turbulent water jet. A row of air jets is used to cool the leading edge of the turbine blades in some jet engines. A machine which automatically joins, straightens, and heat treats continuous railroad track for high speed trains uses air jets for cooling purposes. It is only natural that since this means of surface cooling has become increasingly important that the need for general knowledge about its heat transfer mechanism has increased as well.

Previous to this time Vickers [11]* studied local coefficients of heat transfer from an isothermal heated flat plate

---

* Superscript numbers in parentheses indicate references on p. 79.

to a laminar jet. Gardon & Cobonpue [4] made a similar study for a turbulent air jet over a wide range of Reynolds numbers, nozzle diameters, and vertical distances between the plate and nozzle. However, in a later paper [3] which Gardon co-authored with Akfirat it is stated that the local heat transfer coefficients of Gardon and Cobonpue's original paper are 40 per cent too high. Other papers [5,7] have been written on jet heating but comparison of these results with those obtained from cool jets is difficult because, as the vertical distance between the jet and the plate is increased, the entrainment of atmospheric air rapidly cools the jet, thereby changing the effective temperature difference between the jet and the plate. The temperature of a subsonic room temperature jet, on the other hand, remains virtually constant over its axial length.

It may be seen, then, that there is no completely satisfactory experimental data available on turbulent jet cooling. Also, a perusal of the available literature on jets such as the books by Pai [6], Schlichting [8], and Abramovich [1] reveals that the theory of turbulent jets in its present stage of development is extremely sketchy. There are no universally valid equations available at present which may be directly applied to the local effects of turbulent round jet cooling.

This research on turbulent jet cooling was inspired by an academic interest in the problem as well as by a realization of the practical need for more basic research on this mode of heat

transfer. It was felt that any advancement of the state of knowledge in this field would be of great engineering value.

Data were taken for a turbulent jet over a wide range of Reynold's Numbers (6,000 - 67,000) and vertical distances between nozzle exit and plate. Two nozzle sizes were used to insure generality of the results.

Due to the complexity of the fluid flow problem a theoretical calculation of the local heat transfer coefficients was not feasible. A semi-empirical solution was sought in terms of dimensionless quantities so that the results could be applied to various flow rates, nozzle diameters, and vertical distances between the nozzle exit and cooled surface. Finally, the results of this work were compared, where possible, with the work of previous researchers in this general area.

REVIEW OF PREVIOUS WORK

Heat transfer between round jets and heated flat surfaces has been studied by Vickers [11], by Gardon and Cobonpue [4], and by Smirnov, Verevochkin, and Brdlick [9].

Vickers concentrated on the laminar flow regime where Reynolds Numbers based on properties at the nozzle entrance varied between 550 and 950. Local Nusselt numbers at radial distances from the stagnation point up to three times the nozzle diameter were found to be linear functions of the Reynolds Number. It was stated that this occurs because laminar jets entrain only small quantities of surrounding fluid, thus the scouring action at the boundary layer is directly proportional to the rate of flow. Nusselt numbers at the stagnation point decreased linearly with increasing vertical distance from the nozzle for all flow rates. Within the limits of accuracy of the instrumentation a test was run to determine the minimum value of Reynolds Number for which heat transfer could be measured at the plate surface. At a vertical distance of twelve diameters the minimum Reynolds Number began to drop rapidly, reaching zero at $Z_n/D = 7$. Therefore, at $Z_n/D < 7$ the Nusselt number is a function of the Reynolds Number only. The author made no attempt to explain this phenomenon.

These results provided a valuable contribution to jet cooling technology. They cannot, however, be used to predict heat transfer coefficients in the turbulent flow regime.

In 1962 Gardon and Cobonpue presented an extensive paper on turbulent jet cooling. Local heat transfer coefficients produced by a room temperature turbulent jet ($7000 \leq Re \leq 112{,}000$) impinging on an isothermal, electrically heated surface were measured. Nozzle diameters ranged from .089" to .354". The maximum nozzle velocity was the speed of sound. Using a heat-flow transducer, local coefficients could be determined over a very small area. The results are valuable in that the range of vertical distances was varied from one quarter of a jet diameter to forty times the diameter. Thus data was obtained over virtually the entire length of the free jet, potential cone, transition or mixing region, and finally the region of fully developed flow. The equation:

$$Nu_o = 13(Re)^{0.5}\ D/Z_n$$

Where:
- Nu_o = Nusselt No. at stagnation point
- Re_o = Reynolds No. at nozzle exit
- D = Nozzle diameter
- Z_n = Vertical distance between nozzle and plate

was given as the correlation for the stagnation point heat transfer for $Re > 14{,}000$ and vertical distances between jet and plate greater than twenty diameters.

A correlation of the variation of local heat transfer coefficients with radial distance from the stagnation point for vertical distances greater than ten diameters and Reynolds Numbers in excess of 7,000 was presented in the form of a plot of h/h_o vs. x/Z_n,

Where:
- h = local coefficient at any point on the surface
- h_o = coefficient at the stagnation point
- x = radial distance from the stagnation point

Some interesting phenomenon were observed when the jet was close to the plate ($Z_n/D < 6$). At the stagnation point heat transfer rates rose from $Z_n/D = 0.5$, reached a maximum at $Z_n/D = 6$ or 7, then fell off steadily with increasing Z_n/D. Fig. 1 is a generalized curve showing the variation of stagnation point heat transfer with Z_n/D that was observed by Gardon and Cobonpué. They theorized that this phenomenon is due to the variation of stagnation temperatures along the axis of the jet due to air entrainment.

An unusal variation of local heat transfer rates was also observed in the radial direction for $Z_n/D < 6$ as is shown in Fig. 2. Peaks occuring at $x/D = 0.5$ were attributed to high radial velocities between the plate and the sharp edged nozzle exit. Peaks at $x/D = 2$ were thought to be due to some change in the regime of flow of the spreading stream.

Since the quantitative results of this work are clouded by the fact that the authors later discovered a calibration error in their heat flow transducer (as much as 40%)[4] direct comparison of these results with any others is extremely difficult. A qualitative comparison can and will be made, however, between these results and those which will be presented in this work.

Smirnov, Verevochkin, and Brdlick [9] measured average heat transfer coefficients between a heated plate and a submerged turbulent water jet ($50 \leq Re \leq 31{,}000$) over a wide range of

vertical distances between nozzle and plate. Since no local rates of heat transfer were measured, this paper, although useful for practical application work, offers no new knowledge of the mechanism which controls jet cooling.

Heat transfer between a two dimensional turbulent air jet and an electrically heated, isothermal flat plate was studied by Gardon and Akfirat [3] in 1965. For Reynolds Numbers greater than 2000 and vertical distances in excess of fourteen times the slot width, stagnation point heat transfer coefficients were correlated within $\pm$ 5% by the equation:

$$Nu_o = 1.2\ (Re)^{0.58}(Z_n/B)^{-0.62}$$

Where: B = Slot width

Re= Reynolds No. based on air properties at the nozzle exit. Characteristic length = B

A correlation for the lateral variation of heat transfer rates was obtained for fully developed slot jets $Z_n/B \geq 8$, $(2{,}750 \geq Re \geq 50{,}000)$ in terms of $(h/h_o$ vs. $x/Z_n)$. These curves show a dependence on the Reynolds Number which was not explained by Gardon and Akfirat.

These results, as well as others presented in the paper but not correlated mathematically, may be applied to round jets, but only with extreme care due to the fact that the characteristics of a slot jet are slightly different from those of a round jet. Although the width of both slot jets and round jets increases linearly with axial distance from the nozzle exit, the centerline velocity decay function is different for the two types of jets.

The center line velocity of the slot jets is a function of $Z_n^{-0.5}$. The centerline velocity of the round jet is a function of $Z_n^{-1.0}$.[1] The heat transfer phenomenon is similar, however, and useful comparisons may be made between Gardon and Akfirat's work [3] and the results presented here.

Jet heating of flat surfaces has been studied by K. P. Perry [7] and by G. C. Huang [5].

K. P. Perry studied the heat transfer from a water cooled plate to a turbulent heated air jet. The maximum temperature of the jet was limited to 600°C so that radiation effects would be negligible. Perry's formula for stagnation point heat transfer is:

$$Nu_o = 0.181(Re)^{0.7}(Pr)^{0.33}$$

Unfortunately, Perry measured stagnation point heat transfer rates at only one vertical distance between jet and plate, that is, ten diameters. The radial variation of heat transfer rates was measured at vertical distances of 11, 13, 16, and 19 jet diameters.

One of Perry's objectives in his research was to apply the similarity relationship for free fully developed jets which was found by Hinze and Van der Hegge Zijnen, by which contours of velocity and mass transfer across the jet can be expressed independently of jet size and distance downstream of the cross section under consideration. This similarity criterion was

[1] H. Schlichting, "Boundary Layer Theory", (New York: McGraw-Hill Book Co., Inc., 1960), p. 596.

applied with success. The radial variation of heat transfer coefficients for various jet lengths was correlated in the form of a curve of (h/h_o vs. x/Z_n). This method of correlating lateral heat transfer coefficients has been successfully applied more recently by Gardon and Cobonpue. Since all local coefficients are related to the stagnation value, h_o, and since we are given a correlation for stagnation heat transfer at only one vertical setting, Perry's results may only be applied to a jet where the vertical distance to the plate equals ten diameters.

G. C. Huang studied heat transfer between a turbulent heated air jet ($1000 \leq Re \leq 10,000$) at short vertical distances from the plate ($1 \leq Z_n/D \leq 12$). Therefore, the stagnation point on the plate was located in either the potential cone region or the transition region of the jet. Hole diameters ranged from .125" to .250". Heat transfer was measured on a transient basis using a thermocouple mounted in a 1.0" x 1.0" x 0.25" silver block. The equation:

$$Nu_o = 0.0233(Re)^{0.87}(Pr)^{0.33}$$

is given for stagnation point heat transfer for the range of vertical distances tested.

Huang noted, without explanation, that the stagnation point heat transfer is independent of Z_n/D when $Z_n/D < 6$, but begins to decrease with vertical distance as Z_n/D increases beyond 6.

Research by Gardon and Cobonpue [4] and by Gardon and

Akfirat[3] as well as the results being reported inthis thesis show a rise in heat transfer rate in the potential cone region as vertical distance is increased for turbulent jets. This phenomenon probably did not show up in Huang's work due to the nature of the measuring apparatus used. Heat transfer coefficients were measured over a one inch square area which produced average heat transfer rates rather than local heat transfer rates.

It will be recalled that Vickers observed this same phenomenon, also without explanation, at $Z_n/D<7$. However Vickers was studying laminar jets. This effect which he observed in the laminar regime has been verified by the results of Gardon and Akfirat and will be explained further in this thesis.

Perry and Huang both worked with Heated air jets which traveled through ambient air at much lower temperatures to reach the heat transfer surface. Due to ambient air entrainment these jets cooled rapidly along their free lengths making direct comparison between the results obtained with hot jets and those obtained with cool jets extremely difficult.

THE APPARATUS

The test apparatus used in the experiments described below consisted of an air supply system (Fig. 3) and a heated flat plate assembly (Fig. 4).

Air was supplied by a reciprocating compressor through a filter and drier to a plenum chamber, to which different nozzles could be attached. The pressure drop across a thin plate orifice, designed according to specifications provided in the ASME Power Test Codes [10], was used to calculate the flow rates. The pressure at the entrance to the plenum chamber and the pressure drop across the orifice were measured with U-tube manometers. The temperature of the air was measured with an iron-constantan thermocouple at the entrance to the plenum chamber. The entire nozzle and plenum chamber was fixed vertically, but could be pivoted about a flexible connection at the inlet end to permit alignment.

The heated flat plate assembly consisted of the following:

1. A steam chamber 8" in diameter by 5" high which was partially filled with water. Just above the water level a screen mesh was installed to prevent the water from splashing on the back of the heat transfer surface. The chamber was operated at atmospheric pressure. A safety release was provided by a tube connected to the chamber on one end and suspended in a container of water on the other.
2. A 1000 watt electric heater, which was supplied with energy through a 20 Amp. Variac, generated the steam.

3. The heat transfer surface (Fig. 5) consisted of six .567" thick invar rings which were insulated from each other with silicone rubber. These rings were sandwiched to a .125" thick brass plate, the back of which was in contact with the steam. Thermal contact between the invar rings and the brass plate was made with silicone grease, which was loaded with silver powder.
4. Heat transfer was calculated using temperatures measured with iron-constantan thermocouples. Six thermocouples were installed at the interface of the brass and the invar; one thermocouple coinciding with each ring. A total of fourteen thermocouples were installed .055" below the upper surface of the rings. Temperature differences in each ring were measured directly. Individual temperatures were measured at the brass-invar interface using an ice bath reference junction. Millivolt readings were taken with a Leeds & Northrup Model No. 7552 potentiometer which was calibrated against a standard cell. Figure 6 shows the complete thermocouple circuit.
5. A plywood container insulated with fiberglass encased the entire steam chamber.
6. The entire assembly was mounted on a surface having three adjustable legs which enabled vertical movement as well as leveling of the heated plate.

THE TEST PROCEDURE

At the start of each day during which data was taken, the compressor, the steam chamber, and the potentiometer were turned on and allowed tooperate for one hour before any data were taken. This procedure insured that all operating equipment had reached steady state. During this waiting period the barometer reading for the day was taken and the ice bath was prepared.

A complete series of tests was run for the two nozzles having diameters of .250" and .375". Data were taken with the .250" nozzle at eight different vertical distances from the plate varying Z_n/D from 1 to 50. The .375" nozzle was operated at seven vertical settings, the largest being $Z_n/D = 40$ due to physical limitations of the apparatus. At each vertical setting data were taken for five air speeds varying from Re $\cong$ 6,000 to Re $\cong$ 67,000. Thus a total of seventy-five "runs" were made with the equipment.

Prior to each run the apparatus had to be in perfect alignment. The procedure for vertically aligning the nozzle axis was as follows:

1. Install a nozzle of the required inside diameter.
2. Insert a straight smooth rod of the same diameter into the nozzle. The rod is now colinear with the nozzle axis.
3. Suspend a plumb bob in the vicinity of the rod.
4. Adjust the guy wires until the plumb line and the rod are colinear.

5. Repeat steps 3 and 4 along an axis perpendicular to the one just used.

The flat plate had to be positioned at the proper elevation, leveled, and centered under the nozzle. A graduated metal "square" was used to determine vertical positioning of the plate while leveling was accomplished using a water-in-glass level. The center of the plate was located on the nozzle axis by suspending a plumb line from the center of the nozzle.

At each setting of the apparatus the following measurements were made:

1. Room temperature
2. Air temperature at the plenum chamber inlet
3. Air pressure at the plenum chamber inlet
4. Air pressure immediately before the metering orifice
5. Air pressure immediately after the metering orifice.
6. The temperature at the six radial locations at the brass-invar interface.
7. The temperature difference across each invar ring
   a. Center ring - 1 measurement
   b. Next 2 rings - 2 measurements each
   c. Outer 3 rings - 3 measurements each.

The temperature differences in each ring were measured between the thermocouples installed .055" below the upper surface and the thermocouple corresponding to that ring located at the brass-invar interface.

More than one pair of thermocouples was used in the rings wherever possible. Since the invar had to be drilled and thermocouples placed at the base of holes which were .020" diameter the location of each junction after being installed could not be precisely measured. Furthermore, the air flow pattern could not be perfectly symmetrical. Having more than one junction in all but the center ring allowed the averaging of data which procedure led to more reliable results.

ANALYSIS OF RESULTS - GENERAL

Using the ASME Power Test Code [10] and the measured pressures and temperatures, mass flow rates were calculated for all runs. The properties of the air jet at the nozzle exit were calculated by assuming an isentropic pressure drop between the entrance to the plenum chamber and the nozzle exit. Air density was calculated using the perfect gas law. With this information the Reynolds Numbers based on the properties of the air at the nozzle exit were calculated. The characteristic length used in all determinations of the Reynolds Number was the nozzle diameter.

Local coefficients of convective heat transfer had to be calculated next. Local heat transfer rates could be found since the temperature difference and the distance between the thermocouples were known. Assuming a linear temperature distribution between the front and the back of the rings, surface temperatures on the rings could also be calculated. To determine local coefficients a temperature difference must be used which will enable application of these results to design situations. The local surface temperature was selected as one temperature. The other temperature had to be related to the jet. Two possibilities exist here. Either the nozzle exit temperature or the plenum chamber temperature could be used. Since the axial velocity of the jet decreases to zero upon impact at the plate it was reasoned that plenum chamber temperature of the jet would be the more logical temperature to use. This proved to be the case. Heat transfer rates, as will be shown in detail, correlated

very well at the stagnation point. A typical calculation of the local coefficient of heat transfer is as follows:

$$q = \frac{K}{L_i} \Delta T_i = h \ (T_s - T_j)$$

Solve for the local convective coefficient giving:

$$h = \frac{k \Delta T_i}{L_i \ (T_s - T_j)}$$

Where:

q = Heat transfer per unit area per unit time ($B/ft^2/hr$)

k = Conductivity of invar ($B/hr\ ft\ ^\circ F$)

L_i = Distance between thermocouples

ΔT_i = Temperature drop across the invar

h = Local convective coefficient of heat transfer

T_s = Surface temperature on invar ring

T_j = Jet temperature (stagnation)

All of the variables in the above equation are known except T_s, the invar surface temperature, which must be calculated by the method shown below.

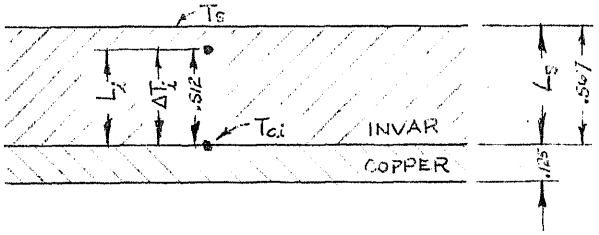

$$T_s - T_{ci} = \Delta T_i \times \frac{L_s}{L_i}$$

$$T_s = \Delta T_i \times \frac{L_s}{L_i} + T_{ci}$$

L_s = Total thickness of invar rings

T_{ci} = Temperature at copper-invar interface

This method of heat transfer calculation has been verified by calculating a heat balance on the entire test apparatus for selected data points. A typical heat balance calculation is included in the Appendix.

ANALYSIS OF RESULTS - STAGNATION POINT HEAT TRANSFER

The problem of heat transfer between a fluid jet and a flat plate perpendicular to it may be considered in two parts. The effect of rate of flow, vertical distance, and nozzle diameter on local heat transfer coefficients at the stagnation point of the jet is an interesting theoretical problem in itself. The variation of the local convective heat transfer coefficients with increasing radial distance from the stagnation point is the other aspect of this problem which will be considered later.

As a first step in analyzing the results of measurements made at the stagnation point a graph of the Nusselt Number (Nu) vs. the dimensionless vertical distance between the nozzle and the plate (Z_n/D) was plotted (Fig. 9). The data for both nozzle sizes were superimposed on the one graph to test the correlation. This general pattern of heat transfer variation at the stagnation point has been observed previously by Gardon and Cobonpue [4] as well as by Gardon and Akfirat [3]. Fig. 10 shows the results obtained by Gardon and Akfirat [3] in their study of two-dimensional jets. When their Reynolds Number is greater than 950 local coefficients of heat transfer rise with increasing vertical distance until the range $4 \leq Z_n/D \leq 7$ is reached. Further increases in vertical distance is accompanied by a rapid decrease in the rate of heat transfer at the stagnation point. This phenomenon is truly remarkable. With the jet flowing at a constant Reynolds Number stagnation point heat transfer rates rise, then fall with increasing vertical distance between the plate and the jet.

Gardon & Cobonpue [4] theorized that this phenomenon is due to a variation of the stagnation temperature of the jet along its axis due to interaction with the surrounding atmosphere. These temperature variations which they reported were not sufficient to cause heat transfer coefficient variations of the magnitude that they measured.

This pattern of heat transfer variations with vertical distance is more likely due to the physical structure of the jet and the mechanics of its interaction with the ambient air which is at rest. As the turbulent air leaves the nozzle it has an established flow pattern. The centerline velocity remains constant for approximately seven jet diameters.[2] This region of constant centerline velocity is known as the "potential cone region". At the interface between this turbulent air and the ambient air there is a highly turbulent mixing region in which ambient air gains momentum at the expense of molecules of air in the jet. Thus, the potential cone region of the jet rapidly narrows, while the total mass rate of flow increases. At a jet length of 6 or 7 nozzle diameters the turbulent mixing region converges on the jet centerline as shown in Fig. 15 (b). Therefore, as the length of the free jet is increased the heat transfer coefficients will increase, reaching a maximum at the tip of the potential cone region ($Z_n/D = 7$) at which point the centerline velocity is still at its maximum value and the region of turbulent mixing has converged. Beyond this point as the vertical distance is increased both the velocity and the level of turbulence decrease rapidly; thus, accounting for the similar fall-off of heat transfer rate.

---

[2] S.PAI, Ph.D., "Fluid Dynamics of Jets", (New York: D. Van Nostrand Company, Inc., 1954), p. 120.

Gardon & Akfirat [3], in their study of two dimensional jets took their data in the laminar regime (Re $\leq$ 1000) as well as in the turbulent regime.[3] Their plot of Nu vs Z_n/D (Fig. 10) reveals another interesting phenomenon.

That is, as the Reynolds Number is decreased the rise in heat transfer within the potential cone region becomes less pronounced until Re = 950 is reached. At this flow rate as well as at lower flow rates the heat transfer rate in the potential cone region remains constant as the vertical distance between the jet and the plate is increased.

This phenomenon is to be expected since the heat transfer rates are so dependent on the structure of the jet. At Re = 1000 the flow is laminar and according to theory the heat transfer rate should be proportional to the Reynolds Number at the surface of the plate.[4] Within the potential cone region the Reynolds Number is the same throughout the range of $Z_n/D \leq 7$. A look at the jet phenomena will reveal why this is so. As a fluid flowing in a tube or nozzle leaves that tube or nozzle and enters the atmosphere it has an established velocity profile. At the interface between this moving air and the stationary ambient air a laminar boundary layer develops. Due to friction, momentum is transfered from the moving particles to stationary particles thus slowing down the particles within the original jet. The boundary layer, as we shall call this region of interaction gradually widens until it

---

[3] J.M.F. Vickers, " Heat Transfer Coefficients Between Fluid Jets and Normal Surfaces", p. 969.

[4] Ibid., p. 969.

has consumed the entire jet. Prior to the time that the boundary layer reaches the centerline of the jet the jet properties remain constant. This region, where jet properties are, as yet, unaffected by the surrounding atmosphere is known as the potential cone region. With further increases in distance from the nozzle the centerline velocity of the jet falls off rapidly. Thus we may say that as we leave the nozzle and move along the axis of the jet we will see, first a region of constant velocity followed by a region of rapid velocity decay. At very low Reynold's Numbers where turbulent effects at the plate are non-existent the heat transfer variation with vertical distance from the plate follows the same pattern.

This is to be expected since the only variables at the stagnation point are the "Reynolds Number of Arrival" (based on velocity of jet as it arrives at the plate and the properties of the air at the nozzle exit) and the stagnation point Nusselt number. Within the potential cone region the Reynolds Number based on the nozzle diameter remains constant as vertical distance is changed; therefore, the Nu remains constant. As the vertical distance becomes greater than 7, the velocity takes a sudden drop and continues to decrease until at some point it will reach zero. The local heat transfer coefficient in the laminar regime follows this pattern quite closely. See Fig. 10 at $Re < 1000$.

As the Reynolds Number is increased, the turbulent regime is entered. Velocities of particles are no longer constant with time. Since individual particle velocities are constantly changing in magnitude and direction we may speak only of average properties.

The magnitude of the RMS deviation of individual particle velocities from the average velocity is a measure of the turbulence of the jet. This turbulence causes a greater amount of the ambient air surrounding the jet to be entrained. The kinetic energy loss along the axis of the jet before it reaches the flat plate also increases with the level of turbulence. Therefore the scouring action of the jet will no longer be proportional to the rate of flow only.[5] Since the heat transfer coefficient at the surface is a function of the scouring action of a jet it is obvious that the "Reynolds Number of Arrival" only is not sufficient to correlate the variations in heat transfer.[6] The degree of turbulence must also be considered. To obtain a complete correlation of results over the entire length of the jet in the turbulent regime it would be necessary to be able to completely describe the local turbulence of the jet mathematically. No such analysis has been found as of yet that covers the entire length and width of the jet. The problem is further complicated by the fact that the turbulence seems to be affected by the nozzle diameter as well.[7] Thus in the turbulent regime the Nusselt Number is affected by the Reynolds Number, the jet turbulence, and the nozzle size. The effect of the turbulent boundary layer surrounding the potential cone region seems to be greatest in the range $4 \leq Z_n/D \leq 14$. Beyond $Z_n/D = 20$ the turbulence has dropped considerably. At $Z_n/D = 20$ the local Reynolds Number alone is the criteria for similarity.

Although the turbulent effects are, as yet, beyond mathematical description, thus limiting our ability to produce a correlation of

---

[5] Ibid., p. 969

[6] Ibid., p. 969

[7] R. Gardon & J.C. Akfirat, "Heat Transfer Characteristics of Impinging Two-Dimensional Air Jets", (Journal of Heat Transfer, Trans. ASME, Series C, Vol. 88, 1966, p. 103).

results at the stagnation point, some significant generalizations may be drawn from the data taken in this work.

The plot of Nu vs. Re (Fig. 11A) for all the vertical settings except $Z_n/D = 7$ and $Z_n/D = 14$ shows the excellent correlation of results achieved with the two nozzles. Since the vertical settings of 7 and 14 nozzle diameters fall in the region of transition between the potential cone region and the fully developed region of the jet the results obtained at these settings were plotted separately in Figures 11B and 11C. It is in this transition region where the boundary layer is merging on the centerline of the jet. The turbulent effects, which seem to be a function of the nozzle size as well as the Reynolds Number, have their greatest effect here. The correlation of the Nu vs. Re cannot be expected to be as precise in this region. Thus it will be noted in Figures 11B and 11C that as the turbulent effects increase with the flow rate the per cent difference between the curves becomes greater. At Re = 7,000 the difference is approximately 7% of the smaller value. At Re = 60,000 the difference rises to 19% of the smaller value at $Z_n/D = 7$ where the velocity and turbulence levels are at there maximum levels. By the time $Z_n/D = 14$ is reached the velocity and turbulence levels have decreased markedly as Figure 12 shows. Thus the results at Re = 60,000 are somewhat improved to a difference of 15% of the smaller value

Replotting all the data for all the vertical settings for both nozzles on log-log paper (Fig. 11D) provided some revealing results. Plots of log $Nu/Pr^{0.33}$ vs. log Re are linear for all the vertical

distances from the jet which were tested. In the potential cone region it may be said, in general, that the variation of vertical distance between the jet and the plate has a relatively small effect on heat transfer. Once the potential cone region is left, however, the local coefficient of heat transfer drops rapidly with increasing vertical distance. It will also be observed that the slope of the curve for the data taken within the potential cone region is less than the slope of the curves for the data taken in the remainder of the jet. This definitely shows that there are two distinct regions of heat transfer which must be analyzed separately.

In the potential cone region one line was drawn through the data points. This line represents an average value of heat transfer which may be expected within the potential cone region $1 \leq Z_n/D \leq 7$. The equation of this curve is:

$$Nu_o = 0.828\ Re^{0.447}\ Pr^{0.333}$$

The percentage of error varies with increasing Re from $\pm 5\%$ at Re = 7000 to $\pm$ 9% at Re = 70,000 due to the increasing effect of turbulence. However, within the wide range of flow rates tested this correlation provides extremely useful information within a margin of error which is acceptable for heat transfer work. With further study of the turbulent jet boundary layer, perhaps this percent of error could be reduced.

The important conclusion to be drawn from the correlation of stagnation point heat transfer rates in the potential cone is that a separate and distinct heat transfer mode exists in the potential cone

region. Turbulent fluctuations which seem to be a function of nozzle size cause the variation of local heat transfer coefficient in the potential cone region. To improve this correlation the turbulence characteristics of a free jet would have to be better understood.

The second heat transfer mode occurs outside the potential cone region.* All of the curves of $Nu/Pr^{0.33}$ vs. Re (based on properties at the nozzle) are parallel to each other. Thus, in the fully developed region of the jet the variation of the heat transfer rate with the Reynolds Number is unaffected by vertical distance. However, at a constant Reynolds Number, the heat transfer rate progressively decreases as the vertical distance is increased. Since the slopes of all the curves of data taken in this region are identical, the physical structure of the jet, as it arrives at the plate must be similar. The properties affecting the heat transfer in this region can only be those which vary along the jet axis. These properties are two: the velocity and the turbulence. Therefore to obtain a correlation of data these properties must be related in some way to a common physical location of the jet. To accomplish this a single curve reflecting the variation of both of these properties along the jet axis was formulated. It was calculated as follows:

The curve of axial velocity decay for a turbulent free jet when Z_n/D is greater than 7 takes the form $\frac{7.0}{Z_n/D}$. This is a widely accepted relationship reported in books by Pai and by Schlichting. The curve of turbulence decay with increasing axial distance takes the form $\frac{C}{e^{kZ_n/D}}$ where C and K are constants.

---

*See Figure 11(D).

It is derived by this author from data illustrated in Fig 5.11 in the book "Fluid Dynamics of Jets" by S. Pai.[6] Individual curves of velocity decay and turbulence decay were superimposed on the same coordinates. The single decay curve as shown in Fig.12 is the result of calculating a weighted average of these above mentioned two curves to produce the best correlation. The resulting equation of the "Velocity and Turbulence Decay Factor" is:

$$F = \left[\frac{0.604}{e^{0.1\ Z_n/D}} + \frac{4.9}{Z_n/D} \right] \qquad (7 \leq Z_n/D \leq 50)$$

The heat transfer correlation curve (Fig. 13) is calculated simply by taking the Reynolds Numbers at the nozzle exit and multiplying them by F. This produces the new variable called the "Reynolds Number of Arrival". All of the data taken in the fully developed region is shown on this correlation curve whose formula is:

$$Nu_o = 0.274\ Re_a^{0.569}\ Pr^{0.333} \qquad (Z_n/D \leq 7)$$

At high Reynolds Numbers of Arrival the accuracy of this correlation is extremely good. For example at Re_a = 30,000 the per cent error is $\pm$ 6 %. At very low Reynolds Numbers of Arrival the accuracy is not as good. At Re_a = 1000 the per cent error is $\pm$ 20%. This accuracy is acceptable considering the physical conditions involved. When the Reynolds Number of Arrival is less than 1500 the minimum distance between the jet and the plate is 30 diameters and the maximum Reynolds Number of fluid leaving the jet is 14,000 when Z_n/D = 50.

Although, as was mentioned before, the slopes of the Nu vs. Re curves are different in the potential cone region and the region of

fully developed flow it is interesting to note that when the correlation curves for the potential cone region and the fully developed flow region are plotted on the same coordinates (Fig. 14) that they intersect and they are nearly colinear. This is a verification of the fact that the velocity and level of turbulence of the fluid when it arrives at the plate, rather than when it leaves the nozzle, is one of the major variables in jet cooling.

It must be emphasized that the correlations of the data taken at the stagnation point of the jet represent all of the data taken without exception. It has been pointed out that the per cent deviation of these data from the correlation curves does vary depending on the configuration of the apparatus. This is due to the fact that no correlation of the jet turbulence with nozzle size and Reynolds Number is available. Therefore in the region of the jet where the turbulence effects are the greatest, namely, the transition region between the potential cone and the fully developed region the accuracy suffers slightly. The variation of turbulence along the jet axis is known, however, and has been used in the analysis of heat transfer in the fully developed region.

ANALYSIS OF RESULTS - RADIAL VARIATION OF LOCAL HEAT TRANSFER COEFFICIENTS

The variation of the local coefficients of convective heat transfer on the flat plate as the radial distance from the stagnation point is increased is a complex problem to analyze. Figure 15 illustrates the reasons why the problem must be considered in two parts. There are two distinct phenomena occuring here. First at $Z_n/D \leq 7$ the potential cone region impinges upon the flat plate, thus the fluid as it moves radially from the stagnation point must pass through a region of high turbulence, before the flow pattern assumes a normal radial pattern. When Z_n/D is greater than 7, on the other hand, the potential cone no longer affects the heat transfer at the surface. The flow pattern is now homogeneous and the turbulence is continually decreasing in magnitude as Z_n/D is further increased. In this regime the fluid flows in a homogeneous medium from the stagnation point to the outer edge of the plate. A correlation based on the parameters h/h_o vs. x/Z_n was tried successfully in this homogeneous regime. The results are plotted in Figure 16. As was mentioned earlier this method of correlation was used originally by Perry [7] and later by Gardon and Cobonpue [4], and by Gardon and Akfirat [3]. A curve has been fitted to these results as follows:

$$h/h_o = e^{-1.56\,(x/Z_n)^{0.75}}$$

where:

h = Local coefficient of heat transfer at any radial position

h_o = Stagnation point heat transfer coefficient

x = Radial distance from the stagnation point

Z_n = Vertical distance between the flat plate and the nozzle exit.

This method of correlation was tested in the potential cone region ($Z_n/D \leq 7$) but it failed. A correlation based on h/h_o vs x/D proved to be successful in this region. This method of correlation produced a family of curves, one for each flow rate. No attempt has been made to develop mathematical expressions to fit these curves which are illustrated in figures 17 through 22. At low Reynolds Numbers (6700) the local convective coefficients fall off rapidly as the radial distance from the stagnation point is increased. As the rate of flow (Re) was increased the heat transfer rate dropped off less rapidly in the radial direction. At Re= 54,000 the effects of turbulence began to affect the results to a much greater extent between x/D = o and x/D = 3.0. Finally at Re = 67,500 the correlation breaks down in the region between x/D = 0.5 and x/D = 2.5. This is due to the high level of turbulence at the interface between thepotential cone and the ambient air, and,as was mentioned before,there is no available correlation which includes the turbulent effects near the nozzle exit. At all rates of flow greater than Re = 6700 the accuracy of the correlation suffers to a greater and greater degree between x/D = 0.5 and x/D = 2.5 as the Reynolds Number increases. This is due to the turbulent effects which are steadily increasing with the speed of the air jet.

SUMMARY OF RESULTS

One of the objectives of this work was to obtain useful correlations of heat transfer data for a round, turbulent jet impinging on a heated flat plate no matter how near or far the nozzle was positioned from it. Prior to this time there has been no correlation available for the use of a turbulent jet striking a flat plate at $Z_n/D \leq 7$. Also, because of the care taken in calculating the local heat transfer coefficients on the segmented plate, which were verifiable by a calculation of the total heat transfer from the apparatus, it is hoped that the local heat transfer coefficients which were obtained contain much less experimental error than the previous results.

The results of the correlations may be stated as follows: To calculate local heat transfer coefficients in the potential cone region of the jet ($1 \leq Z_n/D \leq 7$) the following equation applies at the stagnation point:

$$Nu_o = 0.828\ Re^{0.447}\ Pr^{0.333}$$

To calculate the local coefficient of convective heat transfer at radial points on the flat plate use Figures 17 through 22.

In the fully developed region of flow ($Z_n/D > 7$) the local heat transfer coefficient on the flat plate should be calculated using the following equations:

$$Nu_o = 0.274\ Re_a^{0.569}\ Pr^{0.333}$$

$$F = \left[\frac{0.604}{e^{0.1\ Z_n/D}} + \frac{4.9}{Z_n/D}\right]$$

$$h/h_o = e^{-1.56\ (x/Z_n)^{0.75}}$$

$$Re_a = (F)\ Re$$

Combining these equations produces one equation which may be used to calculate the local heat transfer coefficient at any point on the surface of a heated plate (within the range of data taken) which is being cooled by a perpendicular jet whose vertical distance is greater than seven jet diameters. That equation is:

$$Nu = 0.274\left\{\left[\frac{0.604}{e^{0.1\ Z_n/D}} + \frac{4.9}{Z_n/D}\right] Re\right\}^{0.569}\ Pr^{0.333}\ e^{-1.56(x/Z_n)^{0.75}}$$

APPENDIX

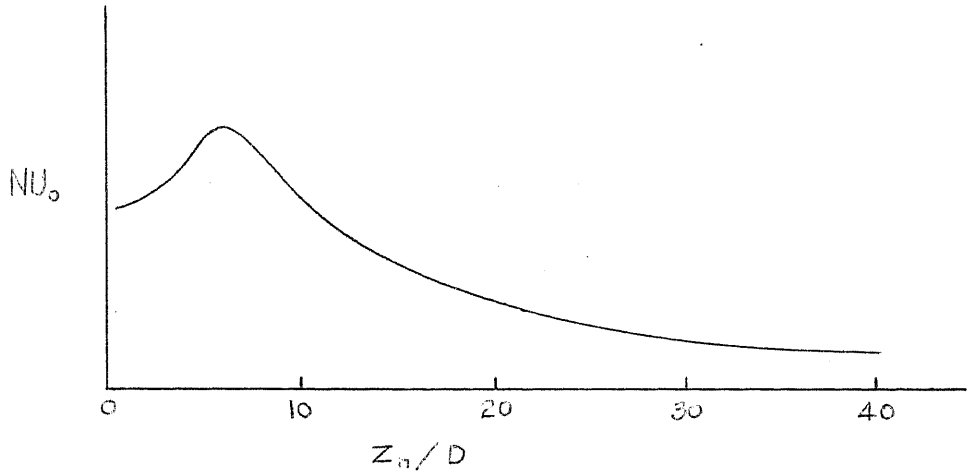

FIGURE 1 - GENERALIZED HEAT TRANSFER VARIATION AT THE STAGNATION POINT DERIVED FROM A RESEARCH PAPER BY GARDON AND COBONPUE.

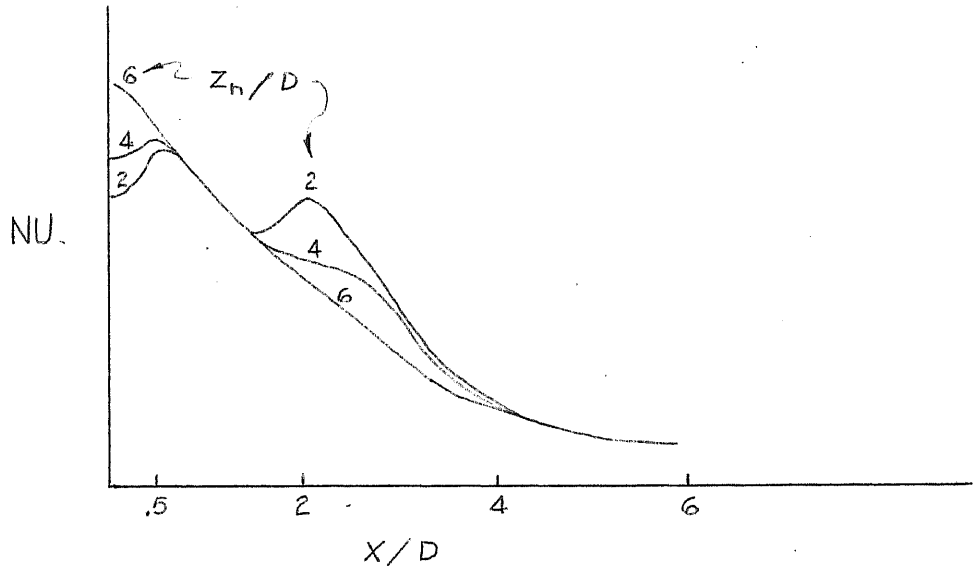

FIGURE 2 - RADIAL VARIATION OF HEAT TRANSFER COEFFICIENTS REPORTED BY GARDON AND COBONPUE.

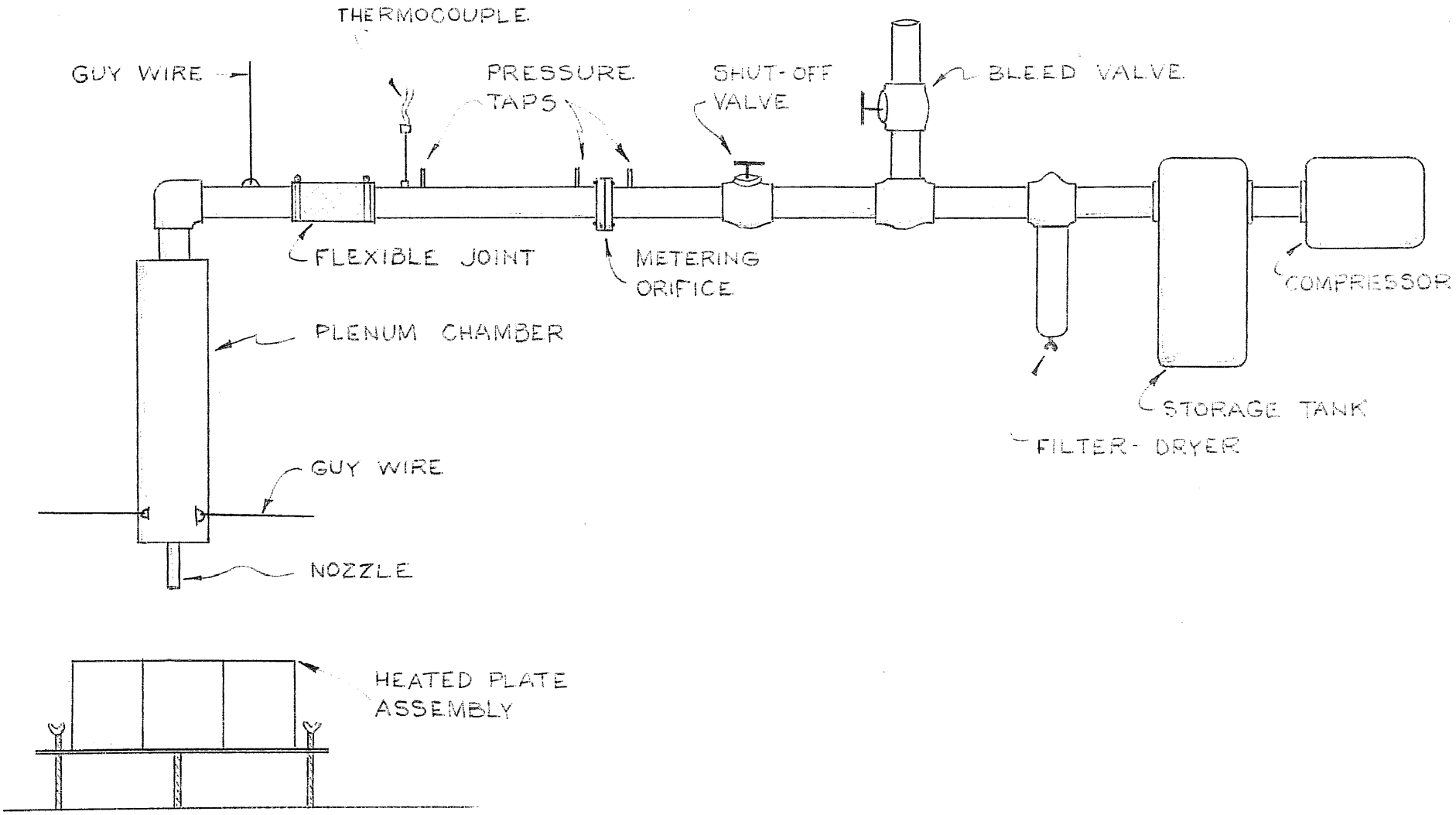

FIGURE 3 - THE AIR SUPPLY AND FLOW METERING SYSTEM

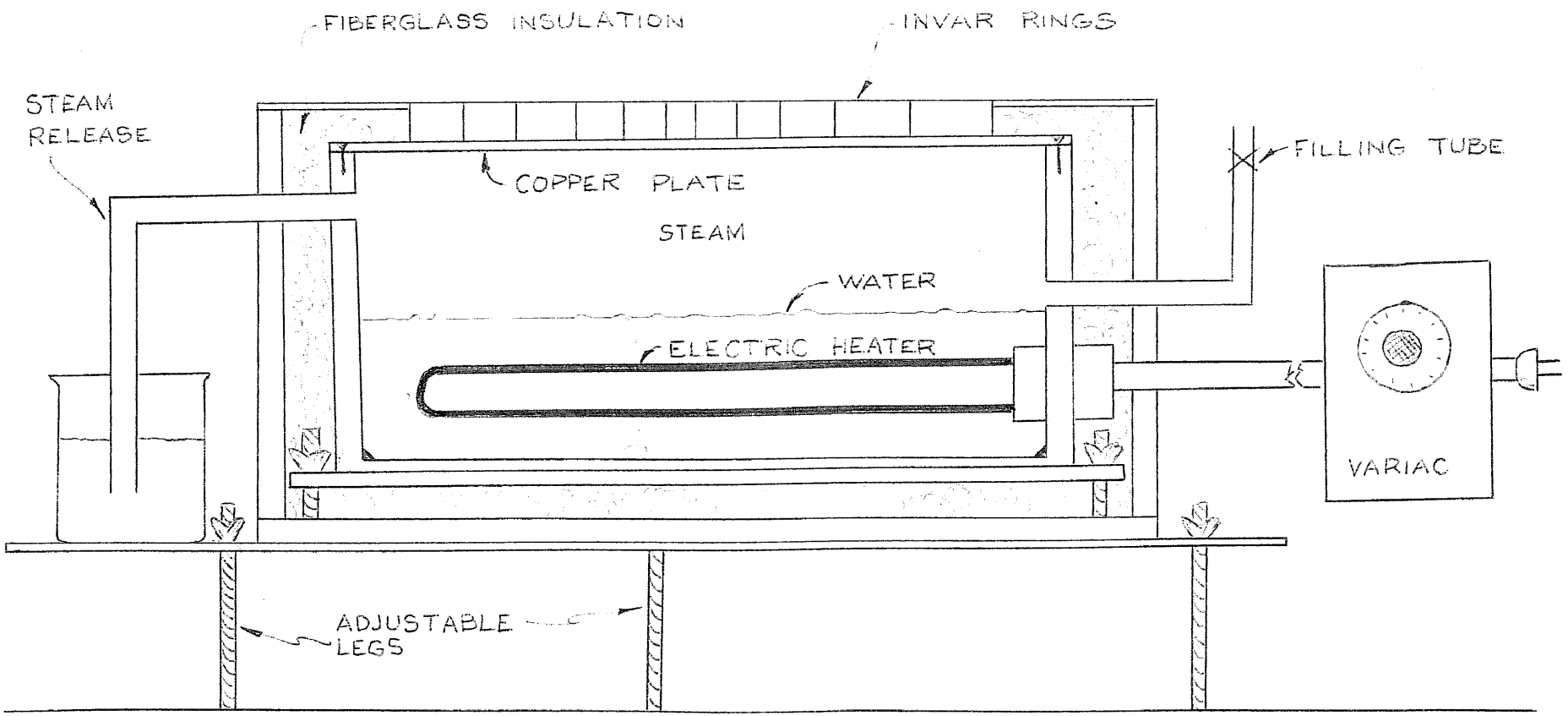

FIGURE 4 - HEATED FLAT PLATE ASSEMBLY

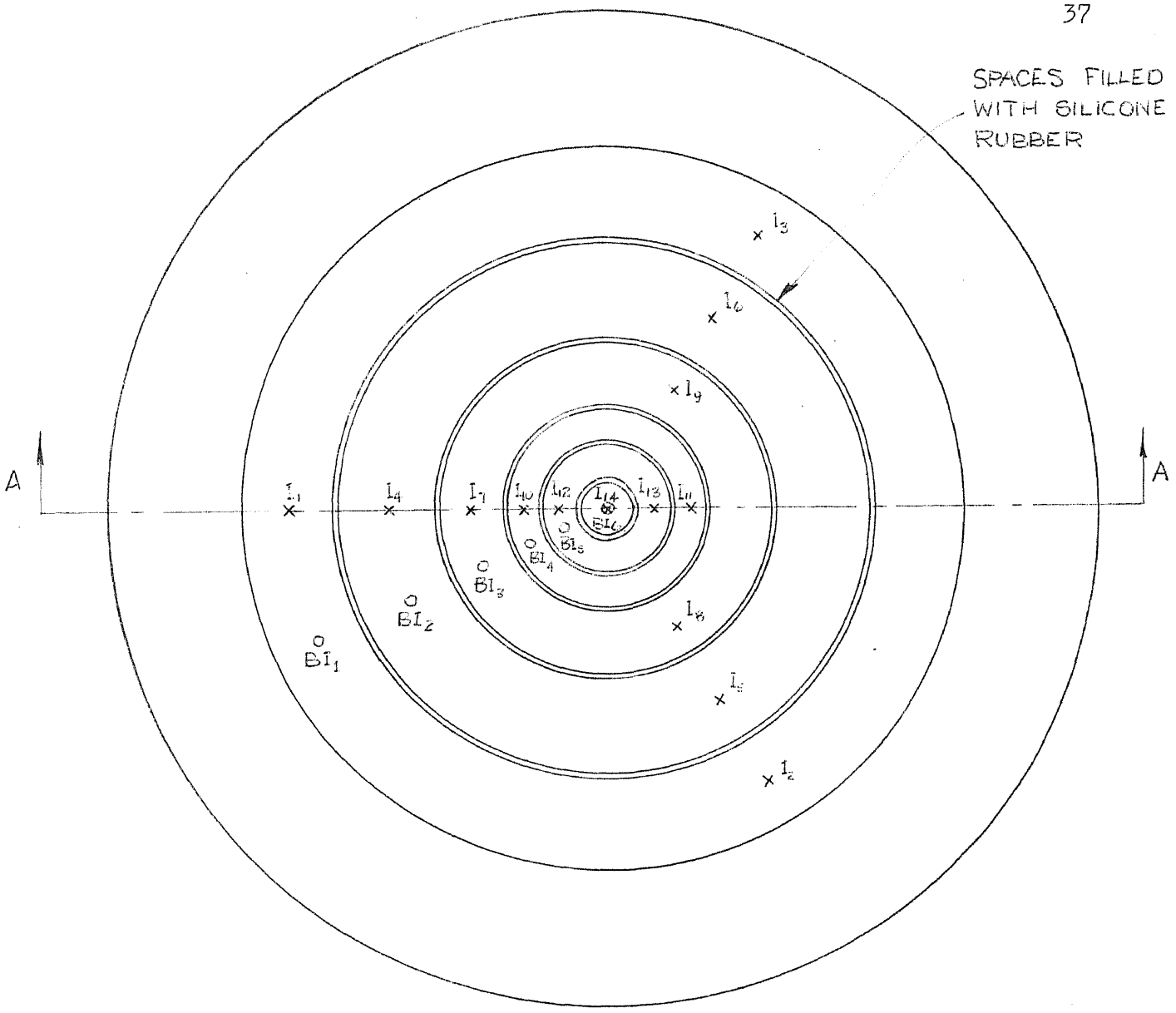

o - LOCATION OF THERMOCOUPLE JUNCTIONS IN BRASS PLATE AT BRASS - INVAR INTERFACE.

x - LOCATION OF THERMOCOUPLE JUNCTIONS IN INVAR RINGS, 0.035" BELOW THE SURFACE.

▨ - INVAR

▨ - BRASS

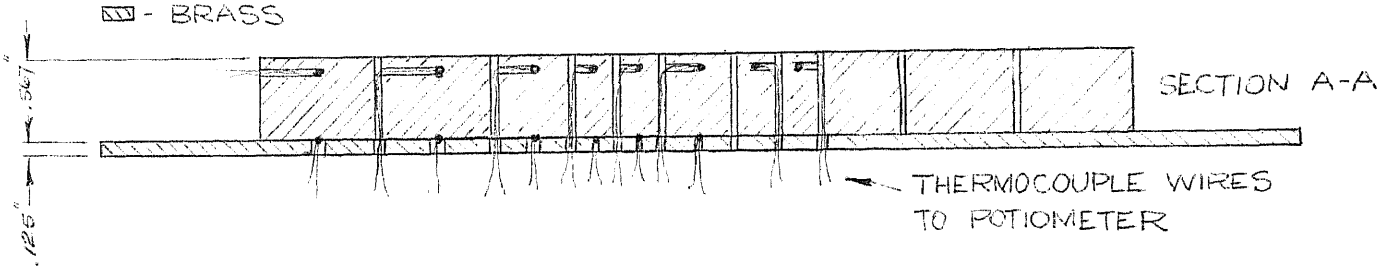

FIGURE 5 - DETAIL VIEW OF THE HEAT TRANSFER SURFACE.

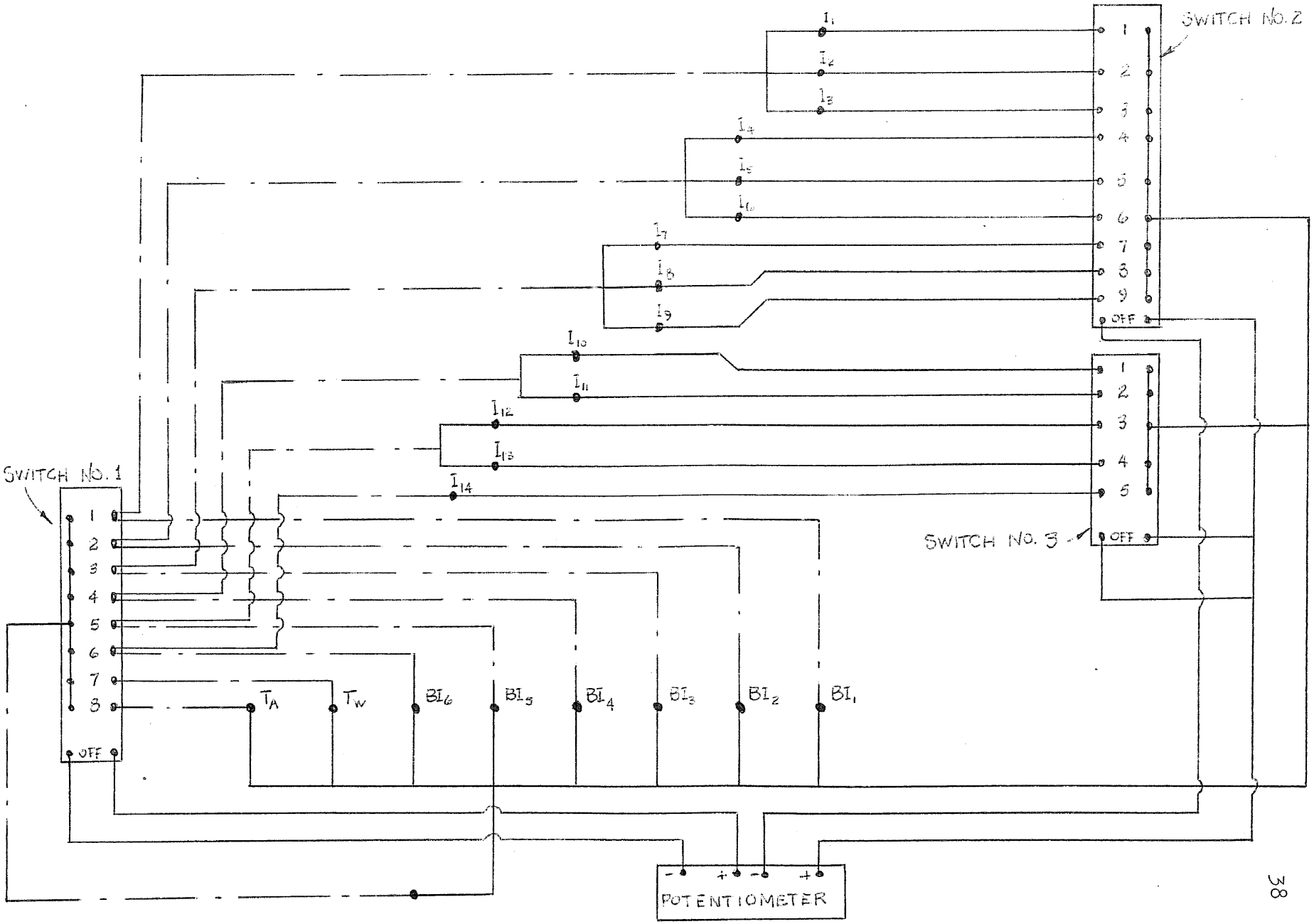

FIGURE 6 - THERMOCOUPLE CIRCUIT DIAGRAM

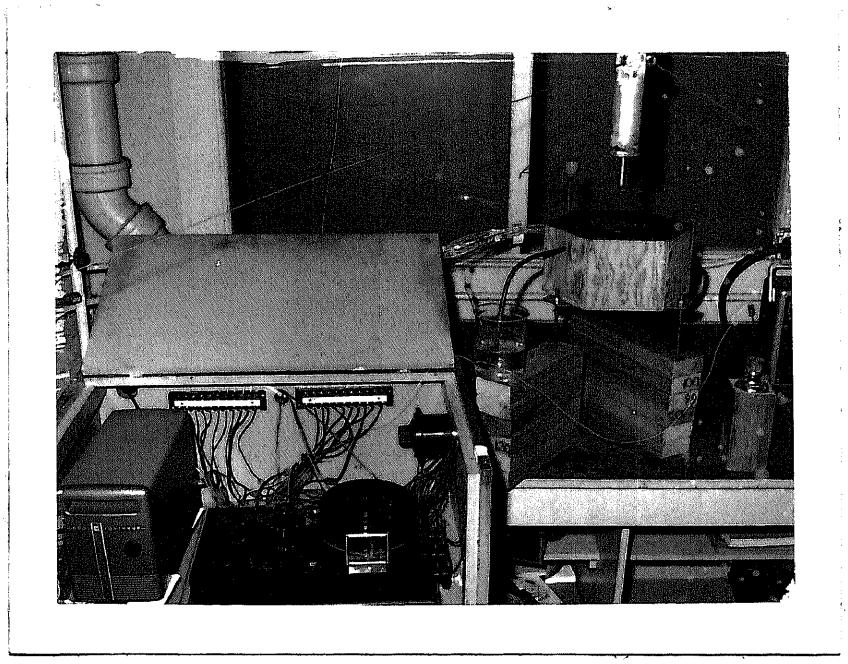

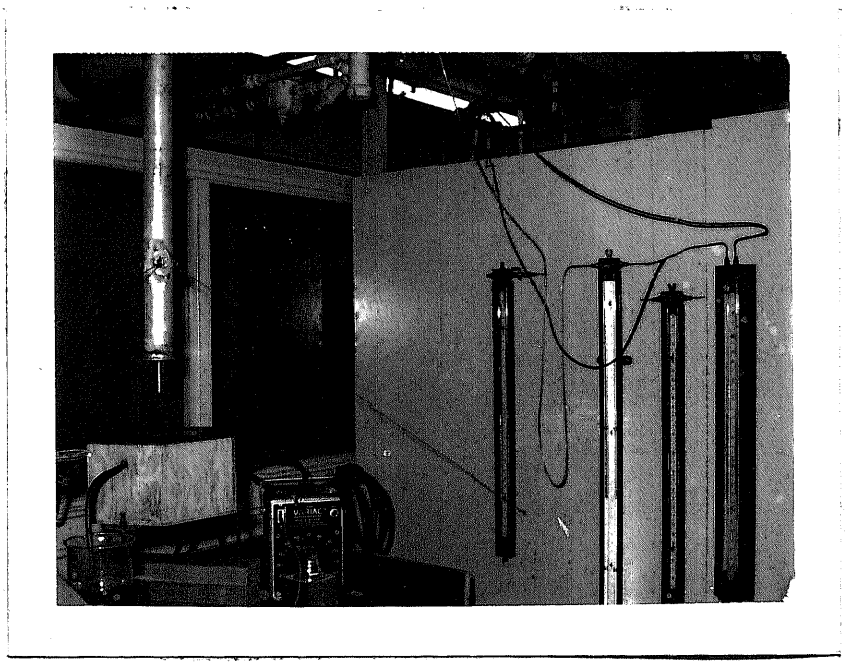

FIGURE 7 - PHOTOGRAPHS OF THE TEST APPARATUS

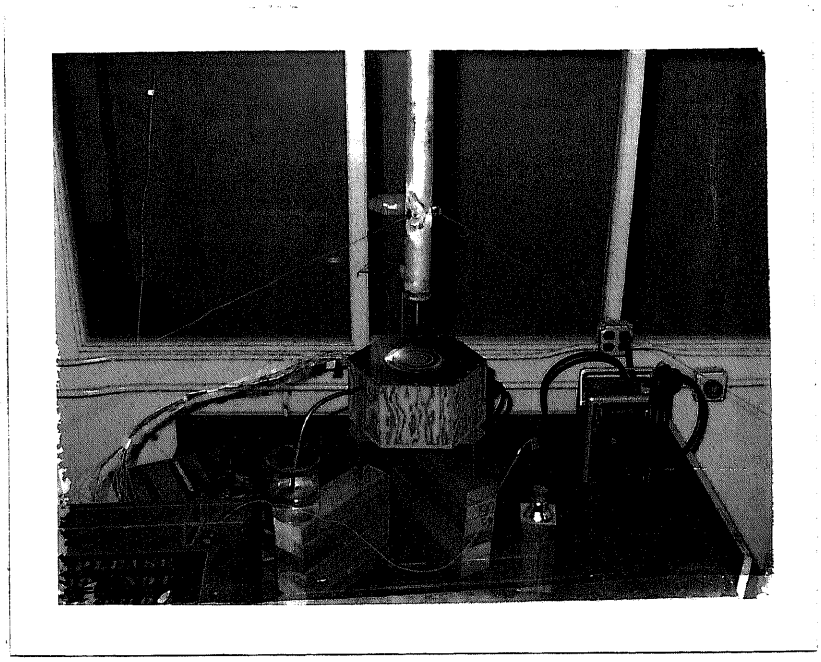

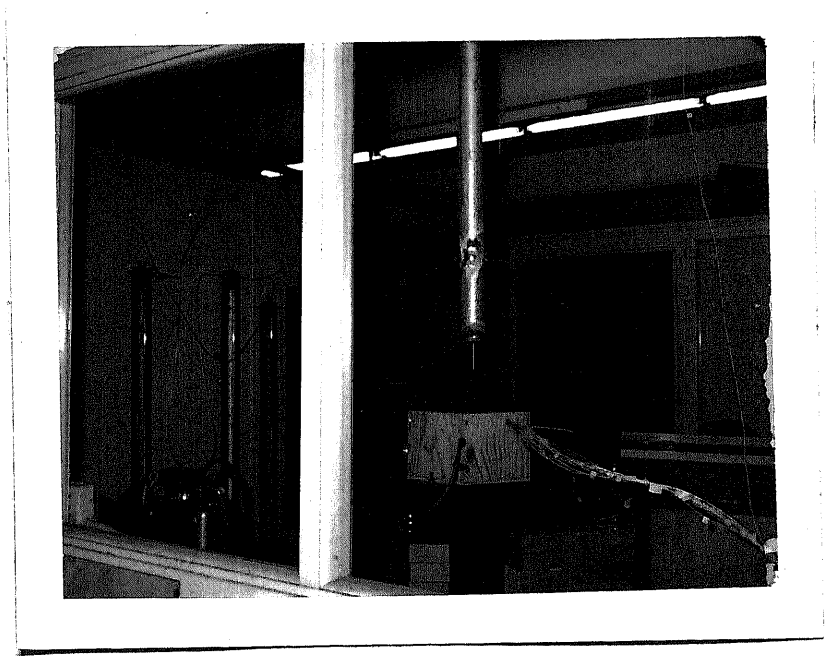

FIGURE 8 - PHOTOGRAPHS OF THE TEST APPARATUS

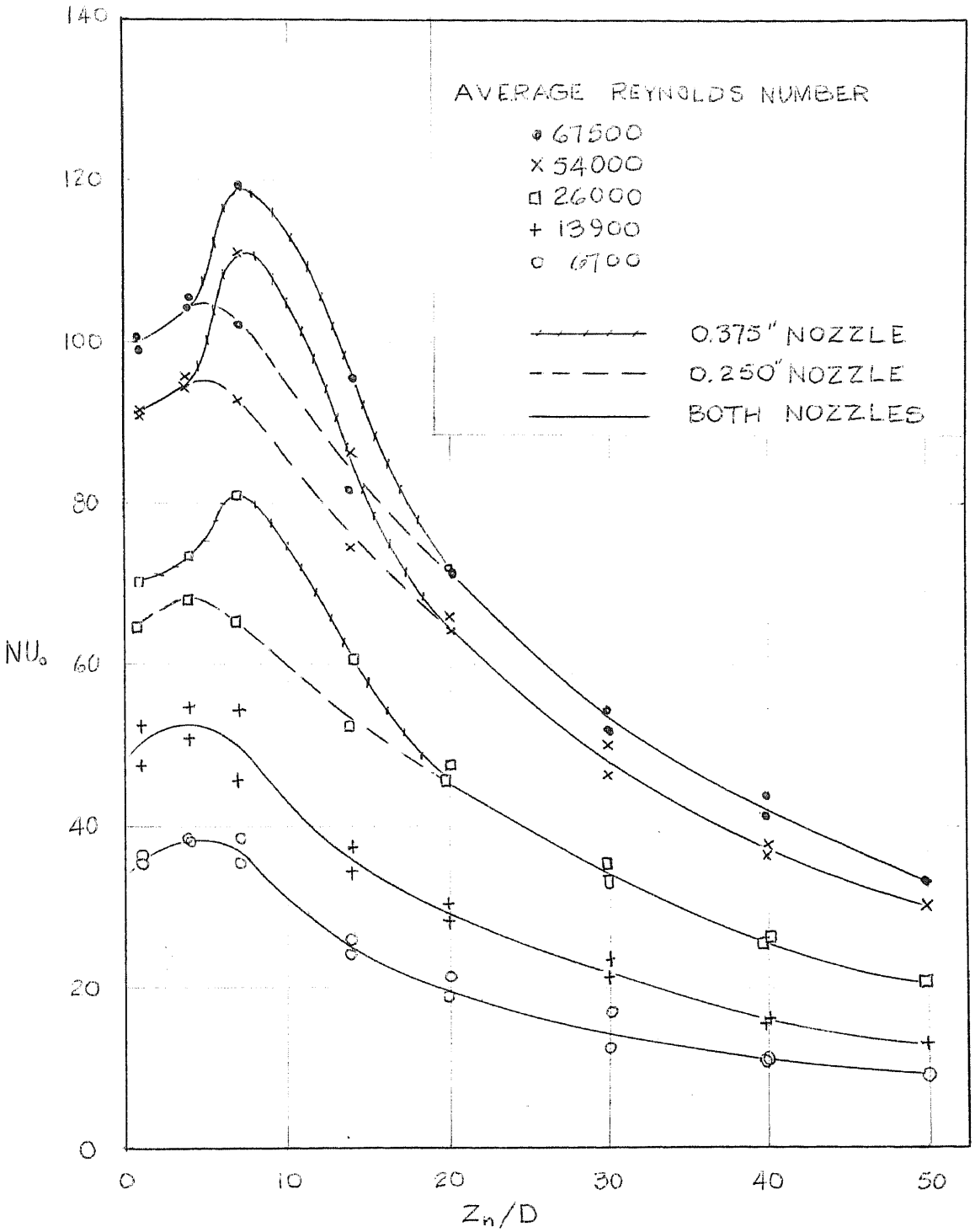

FIGURE 9 - EFFECT OF THE REYNOLDS NUMBER ON HEAT TRANSFER AT THE STAGNATION POINT.

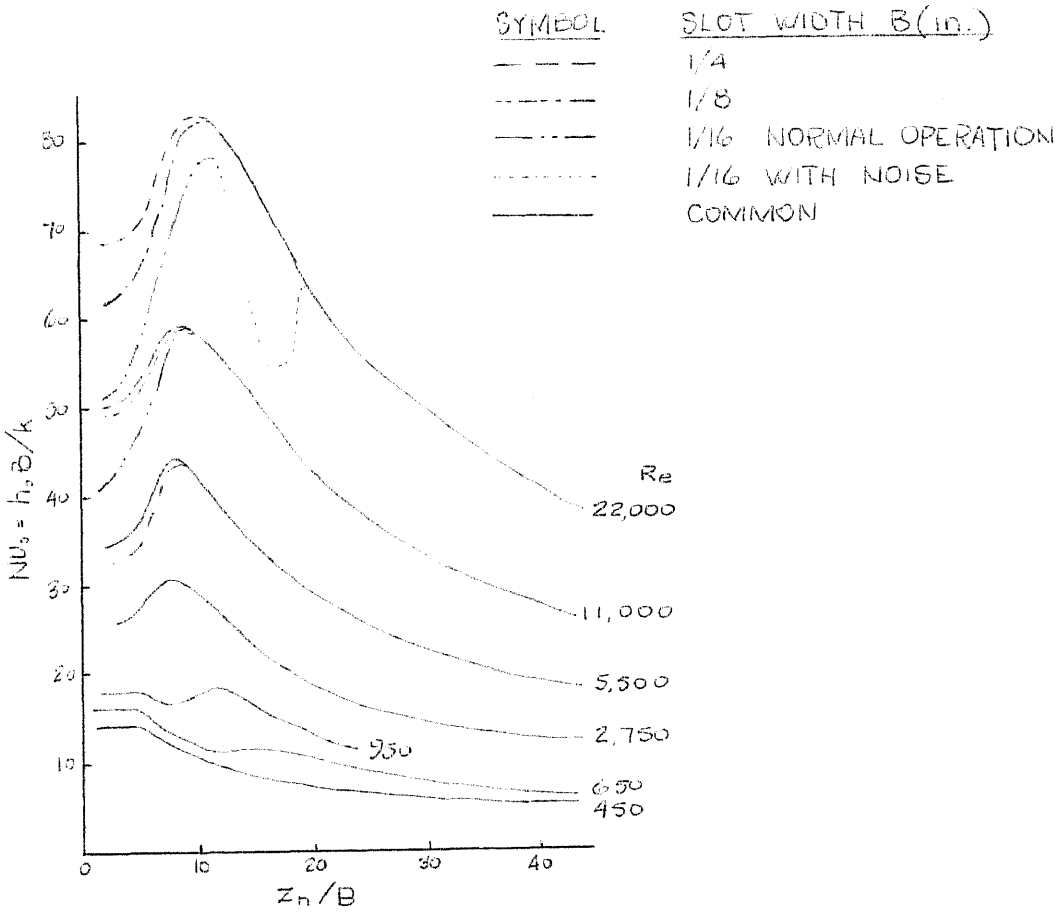

FIGURE 10 - "CORRELATION OF HEAT TRANSFER COEFFICIENTS AT THE STAGNATION POINT OF A TWO-DIMENSIONAL AIR JET". REPRODUCED FROM A RESEARCH PAPER BY R. GARDON AND J.C. AKFIRAT[3].

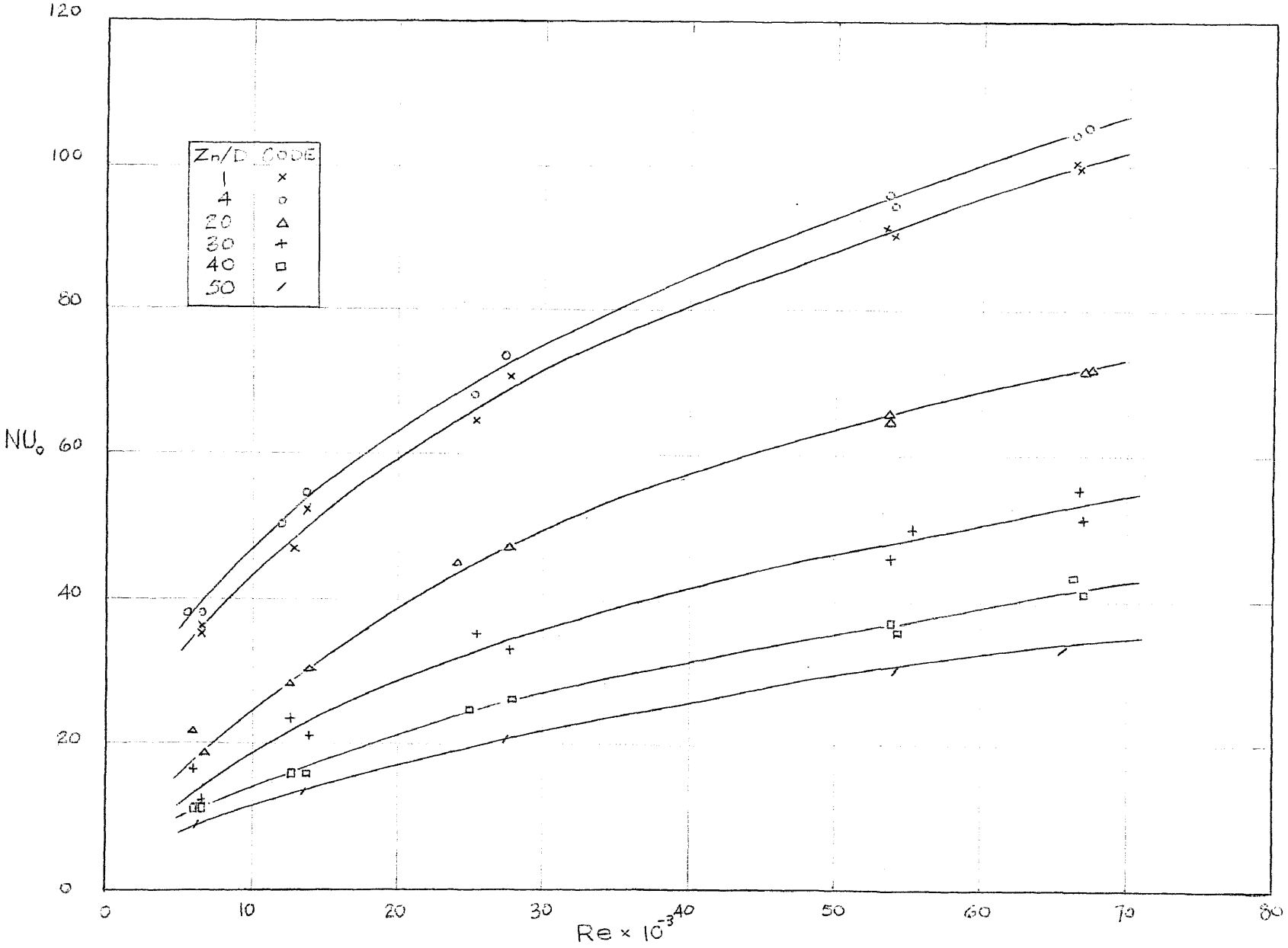

FIGURE 11(A) - NUSSELT NUMBER AT THE STAGNATION POINT VS. REYNOLDS NUMBER BASED ON AIR PROPERTIES AT THE NOZZLE EXIT.

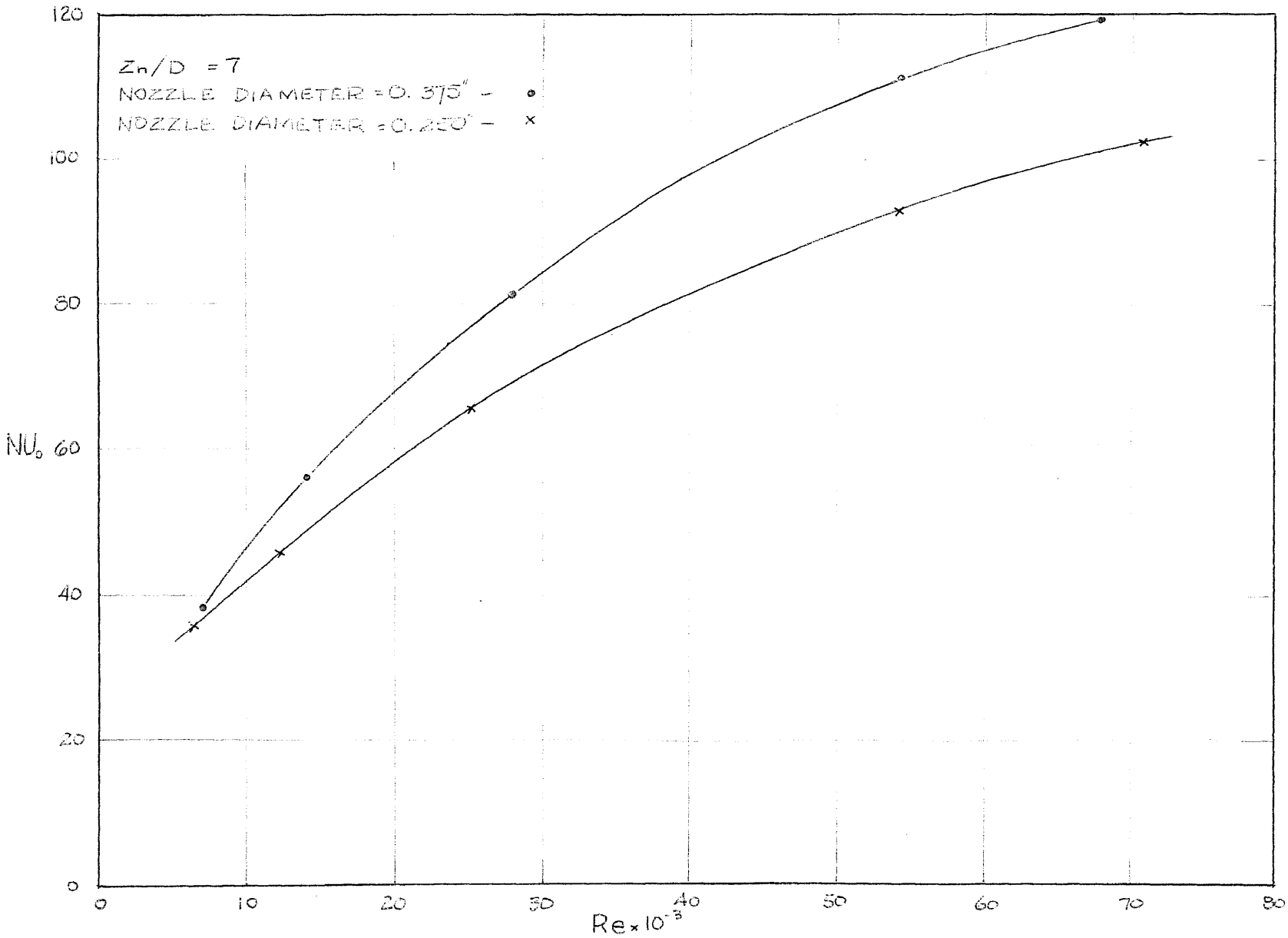

FIGURE 11(B) - NUSSELT NUMBER AT THE STAGNATION POINT VS. REYNOLDS NUMBER BASED ON AIR PROPERTIES AT THE NOZZLE EXIT.

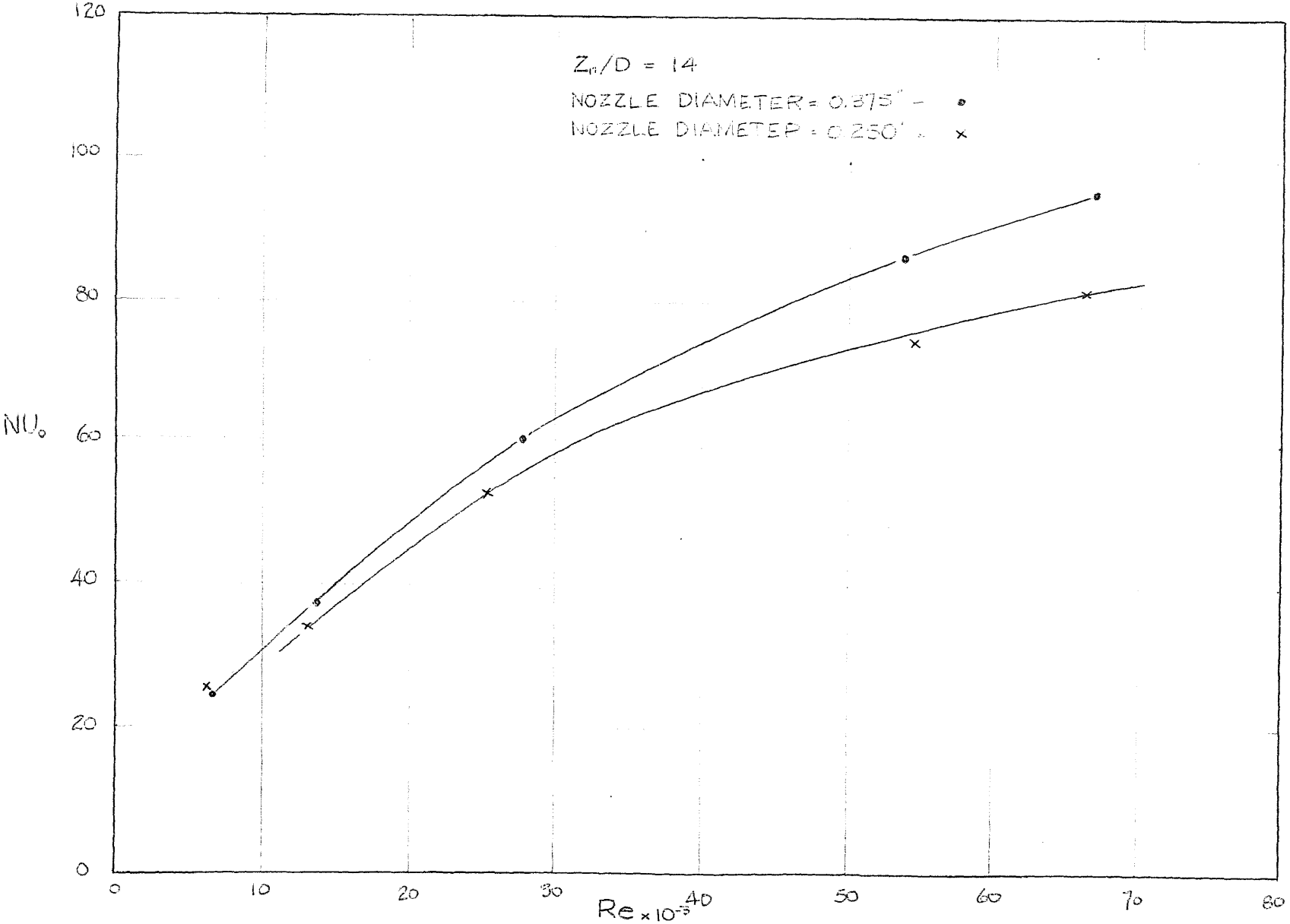

FIGURE 11(C) - NUSSELT NUMBER AT THE STAGNATION POINT VS. REYNOLDS NUMBER BASED ON AIR PROPERTIES AT THE NOZZLE EXIT

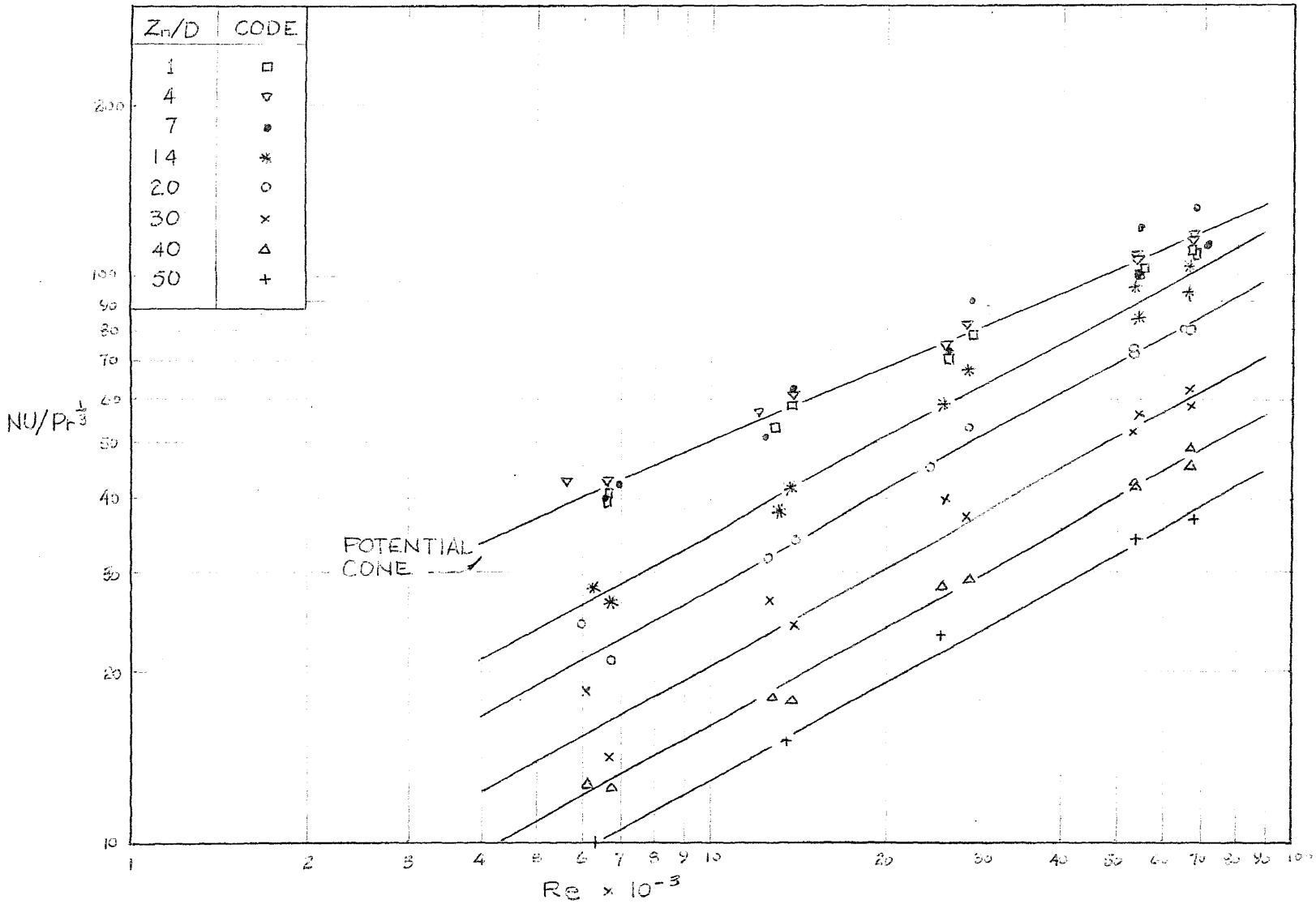

FIGURE II(D) - LOG OF $NU/Pr^{\frac{1}{3}}$ AT THE STAGNATION POINT VS. LOG OF REYNOLDS NUMBER BASED ON AIR PROPERTIES AT THE NOZZLE EXIT.

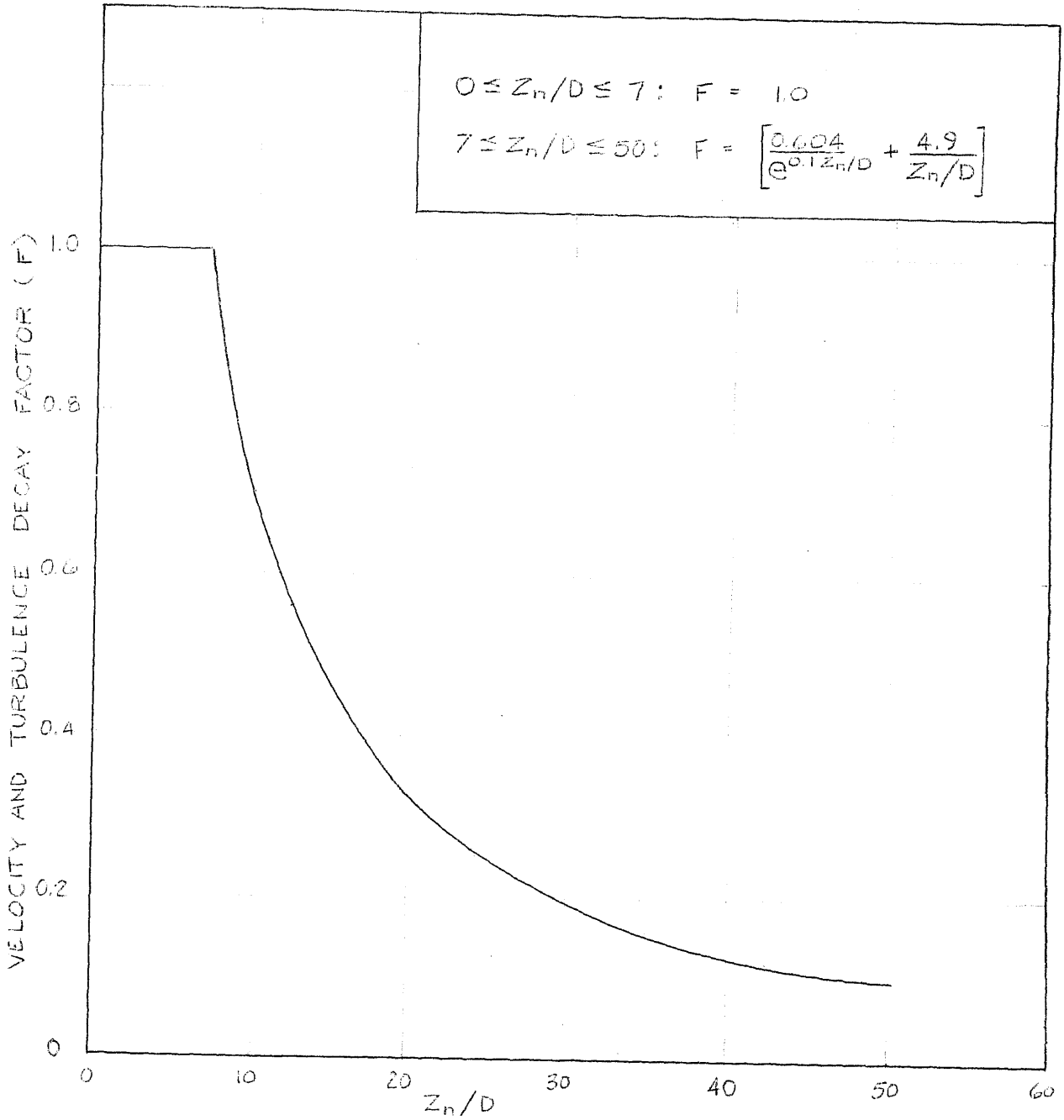

FIGURE 12 - VELOCITY AND TURBULENCE DECAY FACTOR

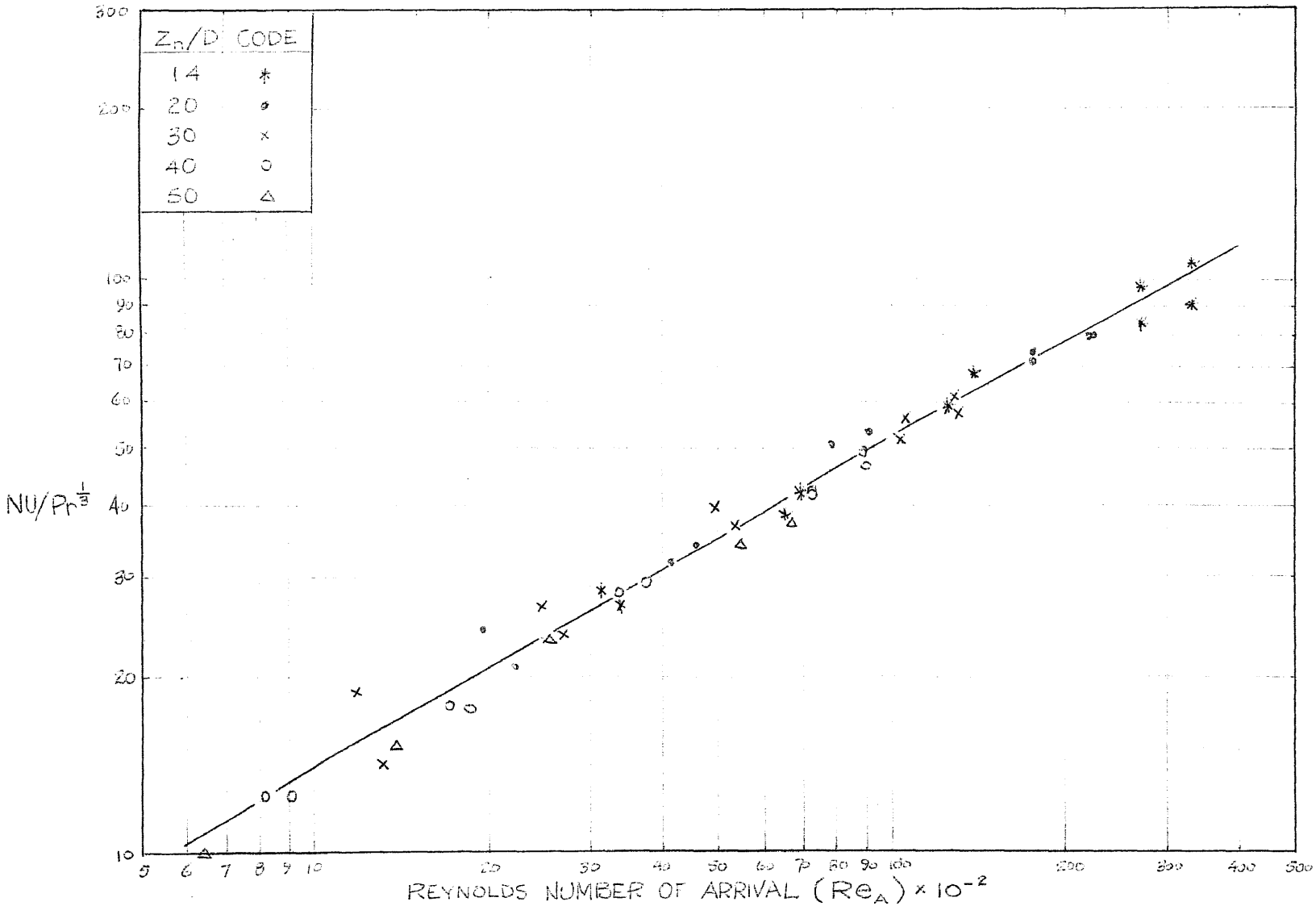

FIGURE 13- CORRELATION OF STAGNATION POINT HEAT TRANSFER FOR $Z_n/D > 7$.

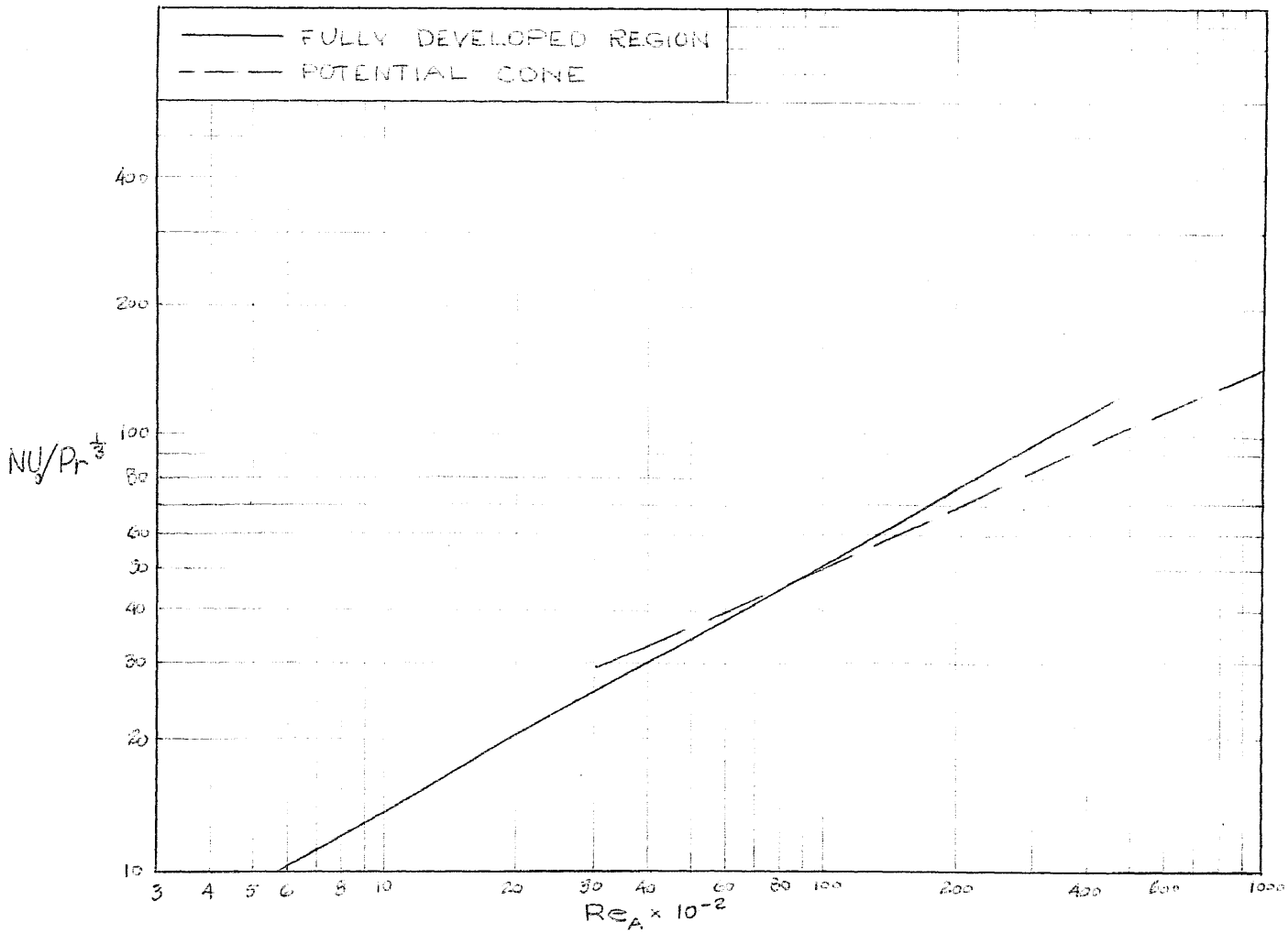

FIGURE 14 - OVERLAY OF STAGNATION POINT HEAT TRANSFER CORRELATION CURVES FOR THE POTENTIAL CONE REGION AND THE FULLY DEVELOPED FLOW REGION.

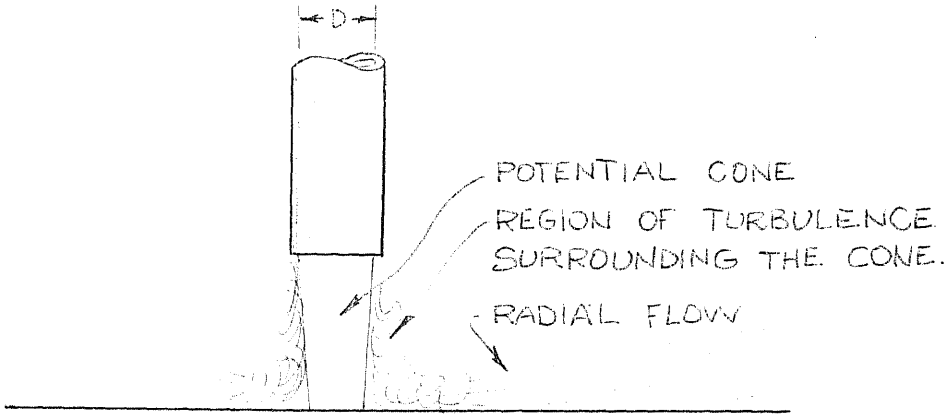

(a) POTENTIAL CONE REGION IMPINGING ON PLATE.

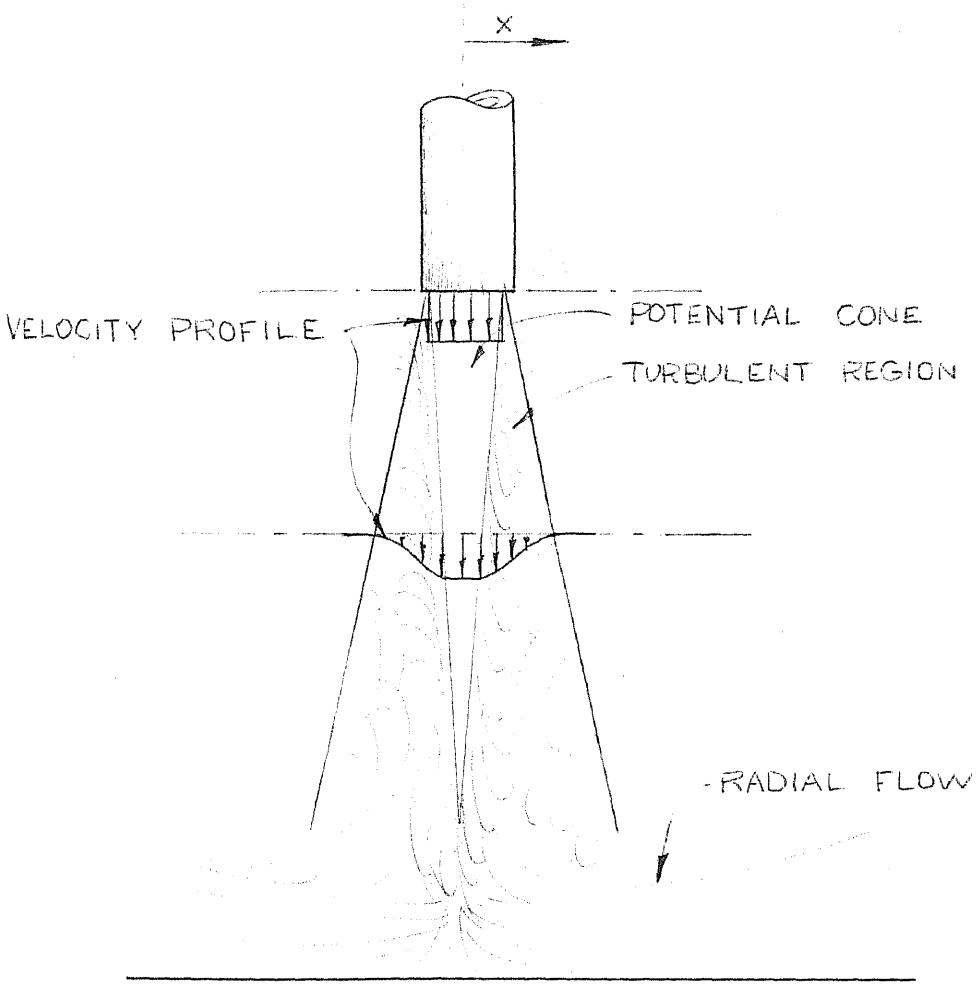

(b) FULLY DEVELOPED JET IMPINGING ON PLATE

FIGURE 15 - ILLUSTRATION OF THE TWO MODES OF HEAT TRANSFER TO AN IMPINGING ROUND JET.

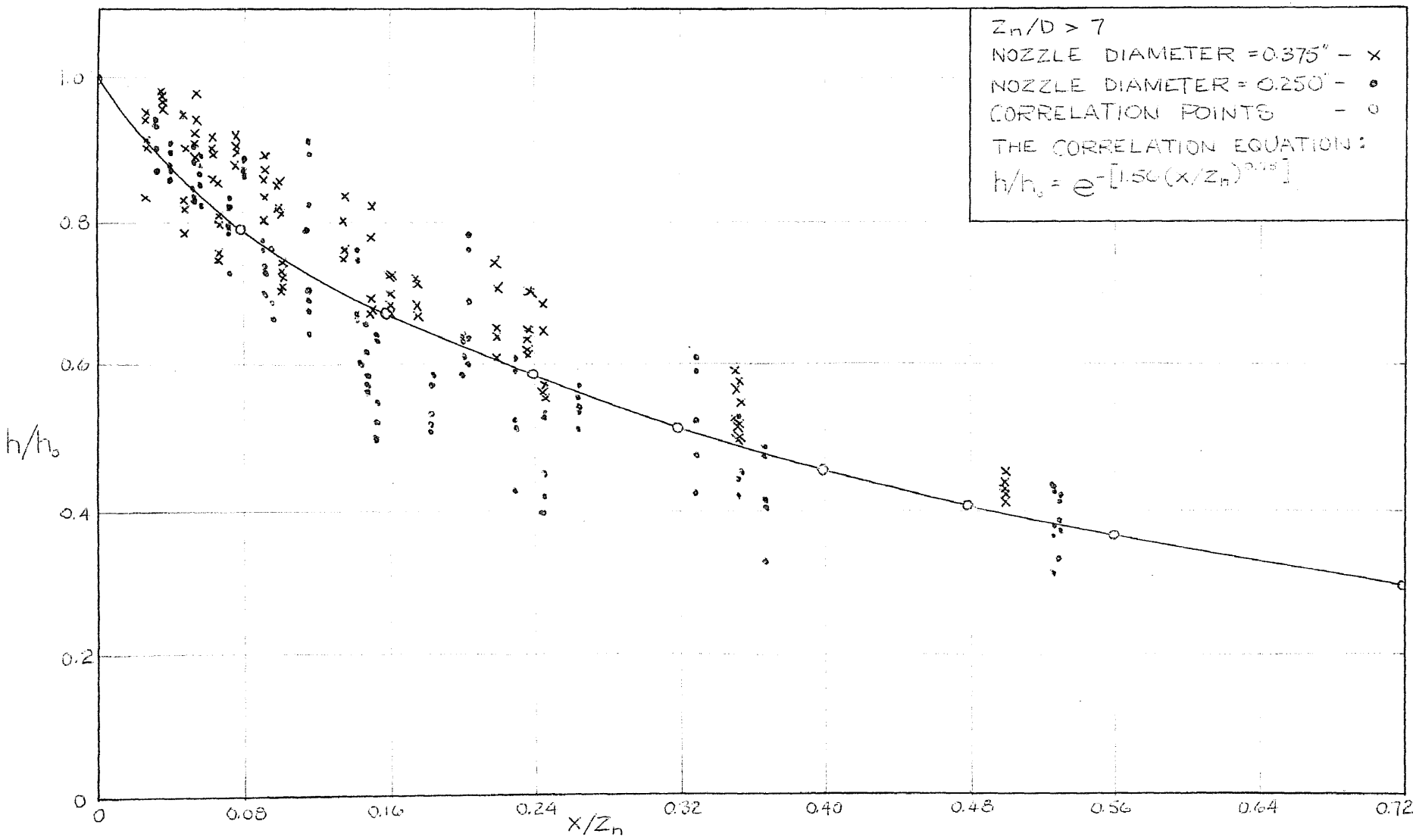

FIGURE 16 - CORRELATION OF RADIAL VARIATION OF HEAT TRANSFER COEFFICIENTS WITH FULLY DEVELOPED JET IMPINGING ON THE FLAT PLATE.

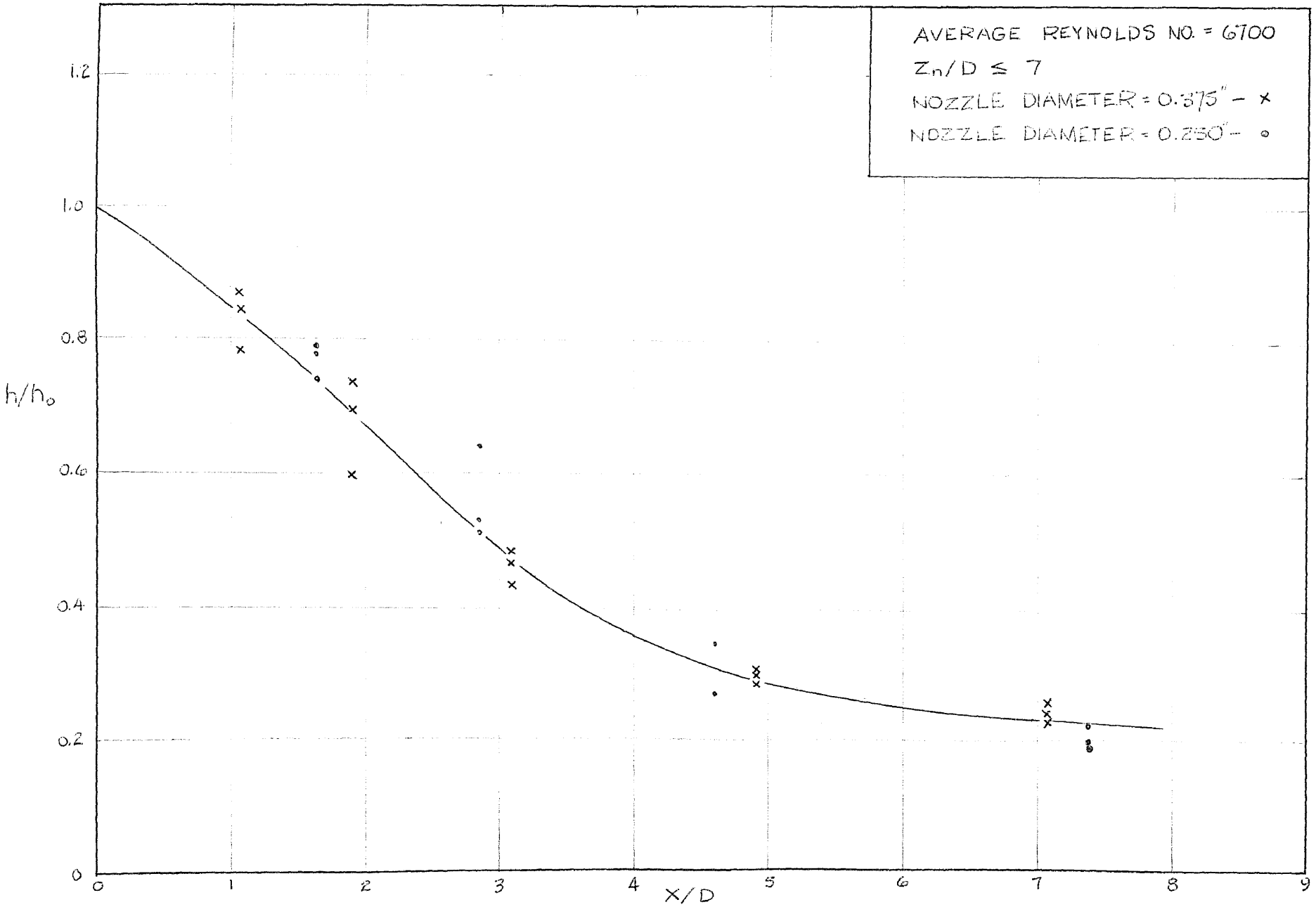

FIGURE 17 - CORRELATION OF RADIAL VARIATION OF LOCAL HEAT TRANSFER COEFFICIENTS IN THE POTENTIAL CONE FOR Re = 6700.

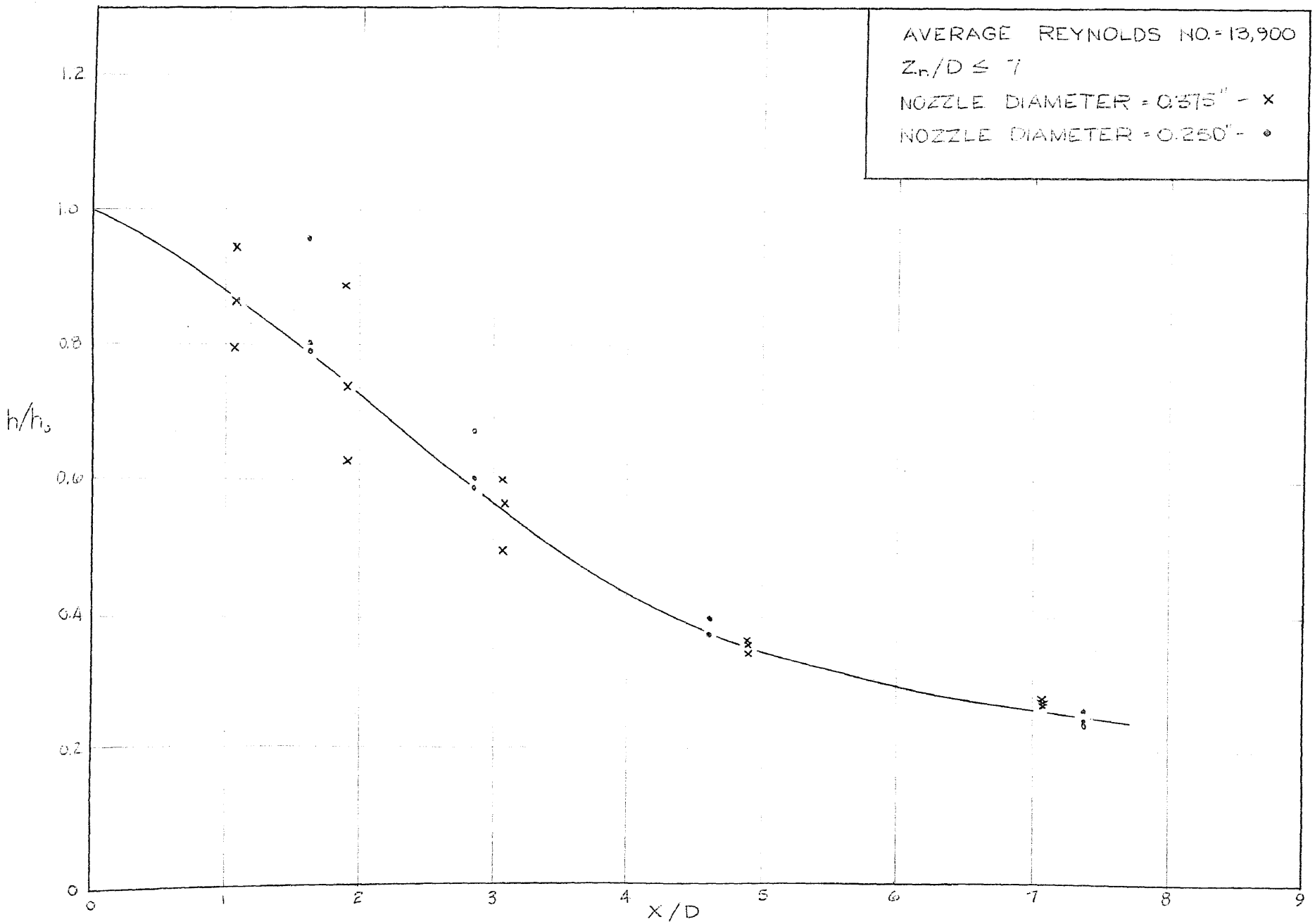

FIGURE 18 - CORRELATION OF RADIAL VARIATION OF LOCAL HEAT TRANSFER COEFFICIENTS IN THE POTENTIAL CONE FOR $Re = 13,900$.

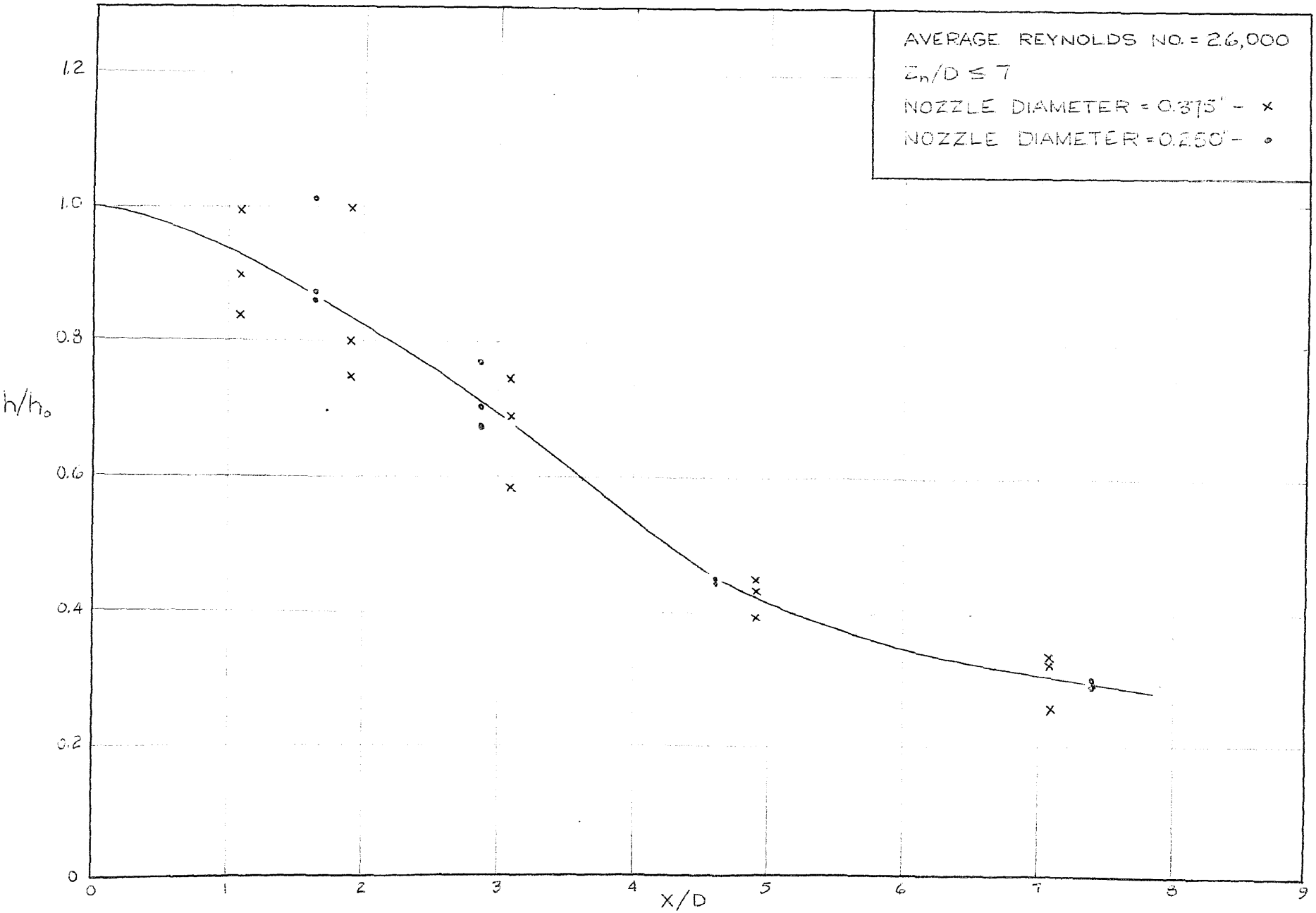

FIGURE 19 - CORRELATION OF RADIAL VARIATION OF LOCAL HEAT TRANSFER COEFFICIENTS IN THE POTENTIAL CONE FOR Re = 26,000.

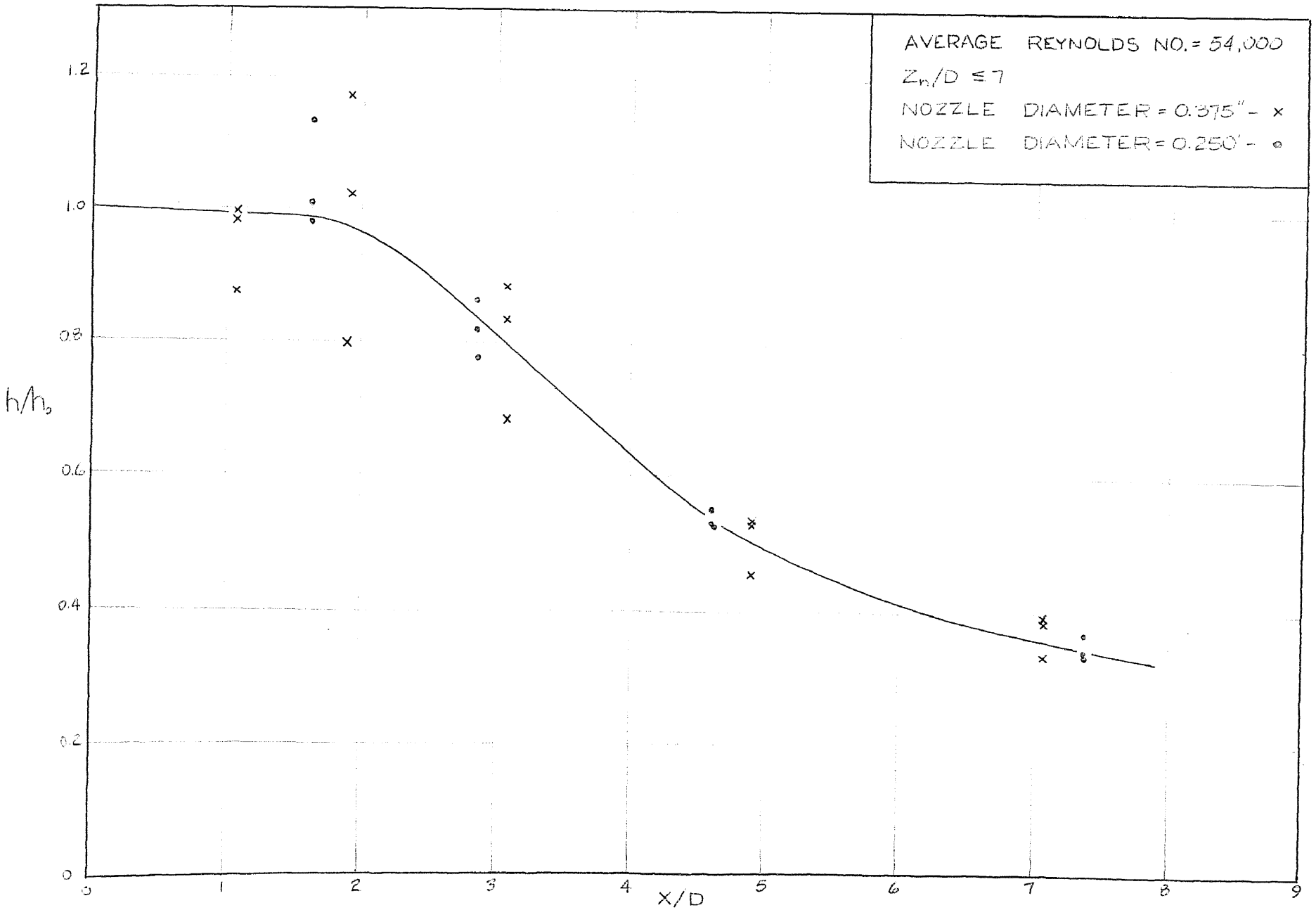

FIGURE 20 - CORRELATION OF RADIAL VARIATION OF LOCAL HEAT TRANSFER COEFFICIENTS IN THE POTENTIAL CONE FOR Re = 54,000.

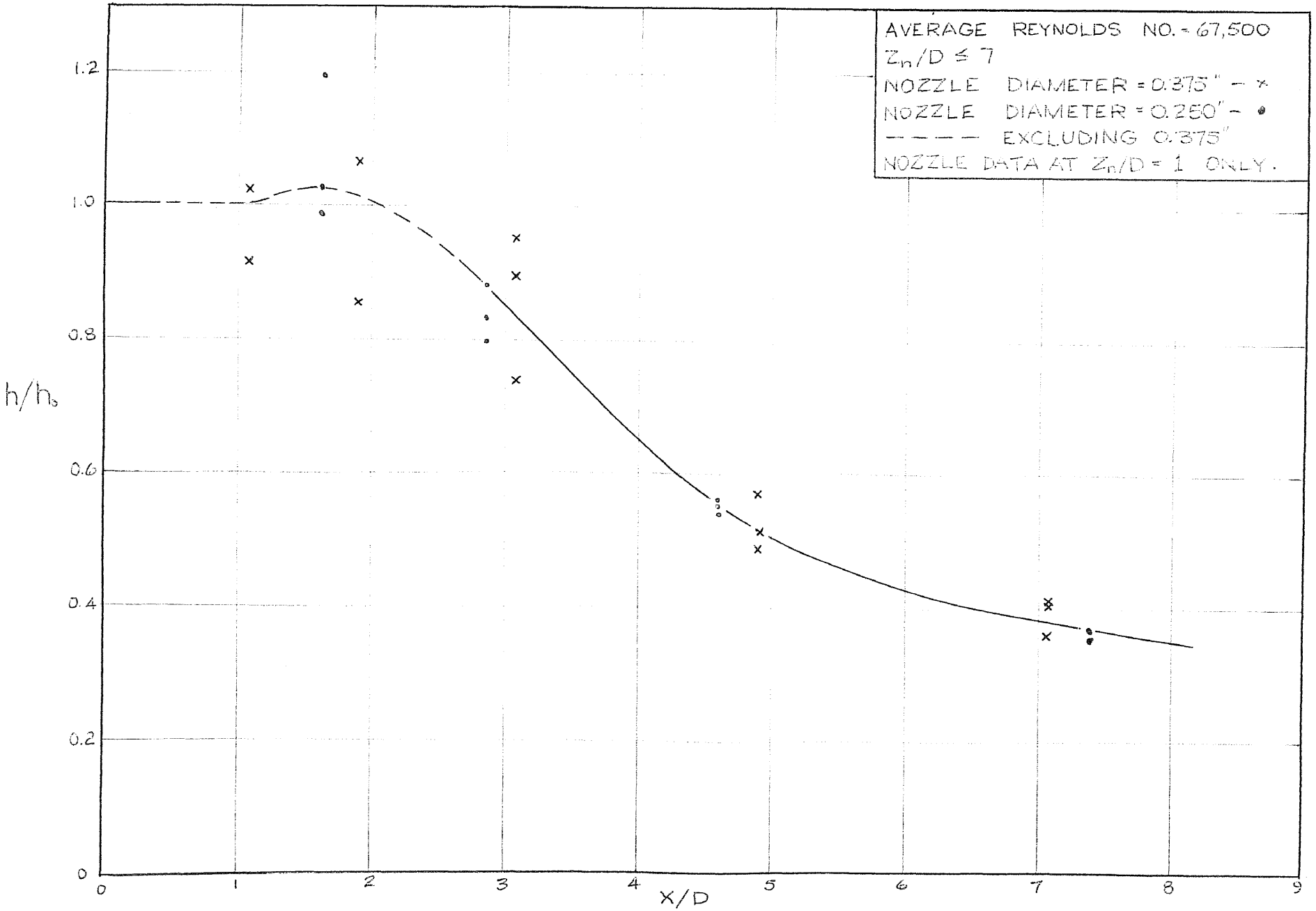

FIGURE 21 - CORRELATION OF RADIAL VARIATION OF LOCAL HEAT TRANSFER COEFFICIENTS IN THE POTENTIAL CONE FOR Re = 67,500.

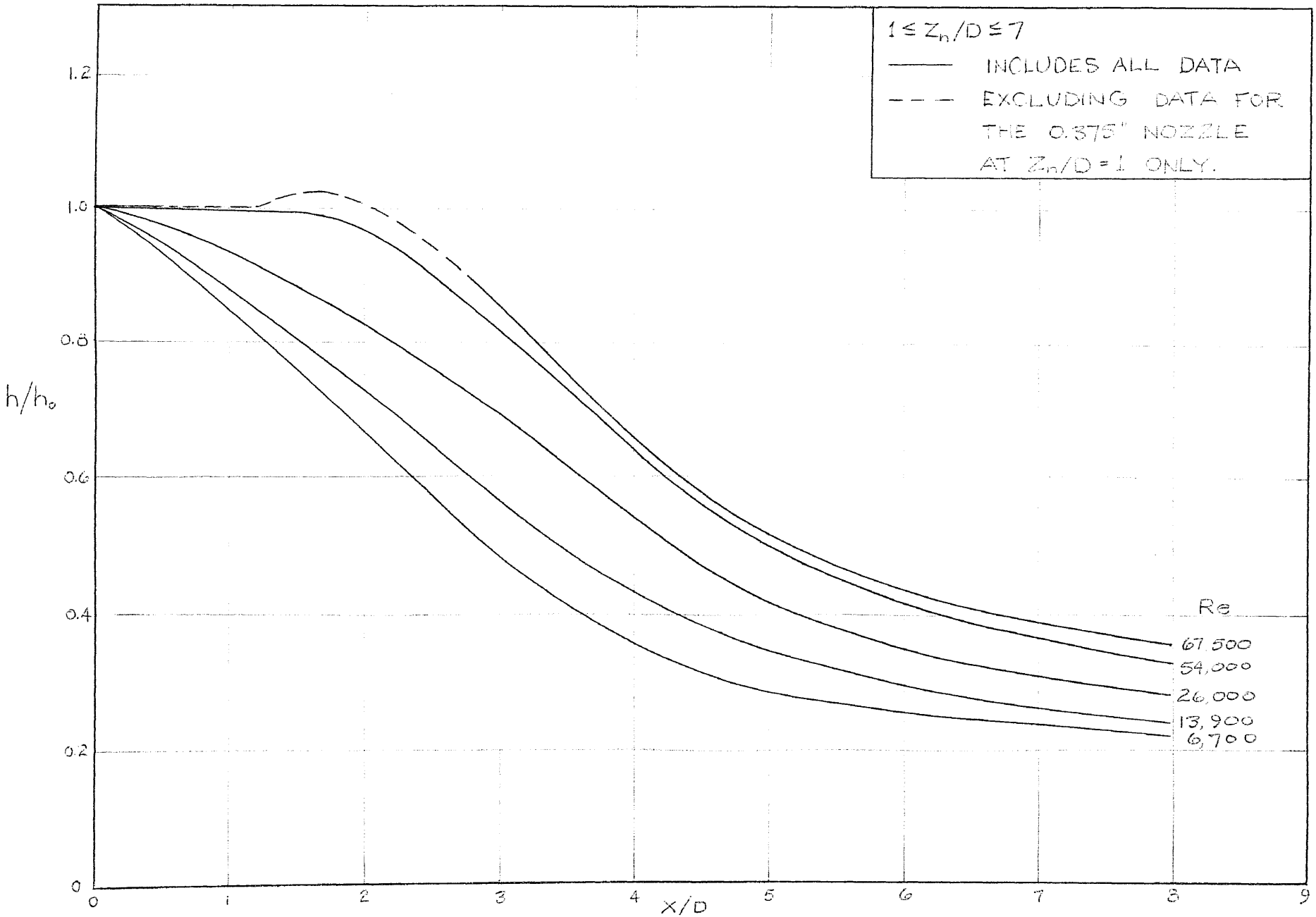

FIGURE 22 - CORRELATION OF RADIAL VARIATION OF HEAT TRANSFER COEFFICIENTS WITH POTENTIAL CONE OF JET IMPINGING ON PLATE.

TOTAL HEAT TRANSFER CHECK

As a means of verifying calculations of local heat transfer coefficients a heat balance was calculated for selected experimental runs. A sample calculation of the heat balance follows:

DATA:

Nozzle Diameter = 0.250 in.

$Z_n/D = 20$

Reynolds Number = 53,727

Heat input = 150 Watts

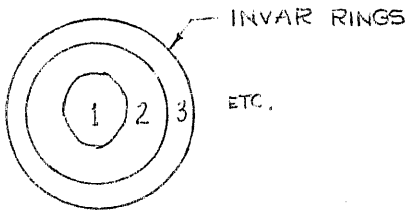

AREAS OF INDIVIDUAL INVAR RINGS:

$A_1 = 1.045 \times 10^{-3}$ ft^2

$A_2 = 4.43 \times 10^{-3}$

$A_3 = 7.88 \times 10^{-3}$

$A_4 = 25.3 \times 10^{-3}$

$A_5 = 6.04 \times 10^{-2}$

$A_6 = 8.67 \times 10^{-2}$

HEAT TRANSFER ACROSS THE TEST SURFACE:

The following values were calculated from the original data:

$$Q = h_1 A_1 T_1 + h_2 A_2 T_2 + h_3 A_3 T_3 + \ldots + h_6 A_6 T_6$$

$$Q = (46.78)(1.045)(10^{-3})(87.64)$$
$$+ (41.54)(4.43)(10^{-3})(89.71)$$
$$+ (34.87)(7.88)(10^{-3})(93.92)$$
$$+ (27.54)(25.3)(10^{-3})(98.87)$$
$$+ (22.03)(6.04)(10^{-2})(103.42)$$
$$+ (19.36)(8.67)(10^{-2})(105.64)$$

$Q = 430.18$ B/hr.

$\underline{Q = 126.2 \text{ Watts}}$

OUTSIDE SURFACE AREAS OF THE INSULATED CONTAINER

$$\text{Vertical Sides} = \frac{(6.375)(6.563)(6) = 1.74 \text{ Ft}^2}{144}$$

$$\text{Bottom} = \frac{(2.598)(6.563)^2}{144} = 0.777 \text{ ft}^2$$

$$\text{Top} = 0.777 - \frac{(\pi)(9.18)}{144} = 0.577 \text{ ft}^2$$

ASSUME:

$k_{insulation} = 0.02$ B/ft hr °f (spun fiberglass)

$k_{steel} = 39.0$ B/ft hr °f

$k_{wood} = 0.062$ B/ft hr °f

HEAT TRANSFER THROUGH THE TOP SURFACE EXCLUSIVE OF TEST SURFACE

Area of Masonite Top = 0.577 ft^2

$$\text{Area of Brass Plate} = \frac{\pi r 2}{144} = \frac{(3.14)(4.25)^2}{(144)} = .394 \text{ ft}^2$$

Area of Plate-Test Area= 0.394 -.20 = 0.194 ft^2

$$\text{Area of insulation} = \frac{394 + .194}{2} + 0.294 \text{ ft}^2$$

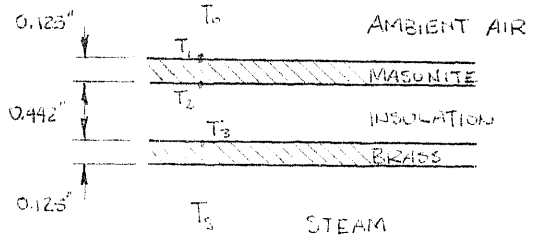

Assume: $T_3 = T_5 = 214°f$

$T_o = 85°f$

$T_1 = 115°f$

$k_{masonite} = 0.07$

$$Q = \frac{T_3 - T_o}{\frac{L_{ins}}{k_{ins} A_{ins}} + \frac{L_m}{k_m A_m} + \frac{1}{h_o A_m}}$$

From Hsu: pg 385:

$h_{top} = (0.38)\ (30)^{0.25} = 0.89\ B/ft^2\ hr\ °f$

$$Q = \frac{214 - 85}{\frac{.442}{0.02 \times 0.294 \times 12} + \frac{0.125}{12 \times .07 \times .577} + \frac{1}{0.89 \times .577}} = 15.2\ B/hr.$$

$Q = hA\Delta T$

$T = \frac{Q}{hA} = (15.2)\ (1.95) = 29.6° = T_1 - T_o$

$Q = 15.2 \times .2931 = 4.45$ Watts

HEAT TRANSFER THROUGH THE SIDES & BOTTOM SURFACES

Thickness of insulation at bottom = 0.68 in.

Average thickness of insulation on the sides = 1.31 in.

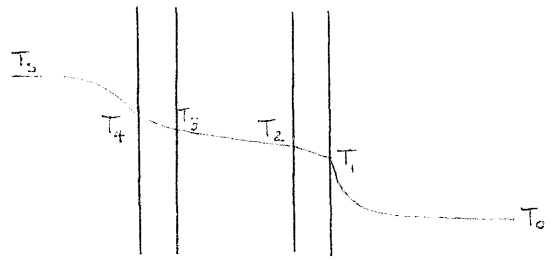

Assume $T_3 = 212°f$

Assume $T_w = 110°f$

$h = (0.28)\ (1.74) + (8.5\quad)\ (4.75) = 0.571\ B/ft^2\ hr\ °f$

$$A_{steel} = \frac{(\pi)\ (4.25)^2}{144} + \frac{(8.5\ )\ (4.75)}{144} = 394 + .881 = 1.275\ ft^2$$

$$A_{wood} = 1.74 + .777 = 2.52 ft^2$$

$$A_{ins} = \frac{1.28 + 2.52}{2} = 1.9 ft^2$$

Average Thickness of Ins. $= \frac{0.68 \times .777 + 1.31 \times 1.74}{2.52} = 1.11$ in.

$$Q = \frac{T_3 - T_o}{\frac{L_{ins}}{k_{ins}\ A_{ins}} + \frac{L_w}{k_w\ A_w} + \frac{1}{h_o\ A_w}}$$

$$Q = \frac{210 - 85}{\frac{1.11}{(0.02)(12)(1.9)} + \frac{.375}{(12)(.062)(2.52)} + \frac{1}{(0.571)(2.52)}} = 37.5\ B/hr.$$

$Q = 37.5 \times 2931 = 11.0$ Watts

HEAT LOSS FROM THE STEAM ESCAPE TUBE

Assume:

$h_o = 0.5$

$k_r = k_{rubber\ ins.} = 0.20$ B/ft hr °f

Tube:

$$Q = \frac{t_i - T_o}{\frac{L_r}{k_r\ A_r} + \frac{1}{h_o\ A_o}} = \frac{127}{\frac{1}{\frac{(r)(.20)(\pi)\ (1.0)(10)}{(144)}} + \frac{1}{\frac{(0.5)(\pi)(1.25)(10)}{(144)}}}$$

$Q = 13.7$ B/hr.

$Q = 13.7 \times .2931 = 4.02$ Watts

Total Watts in = 150.00

Total Watts out = 126.2
4.45
11.00
4.02
145.67 = 146 Watts

$$\% \text{ Error} = \frac{4}{150} \times 100 = 2.7\%$$

ORIGINAL DATA

Nozzle Diameter - 0.250 in.
Vertical Setting, Z_n - 0.260 in.
Approximate Z_n/D - 1
Barometric Pressure - 30.446 in. Hg.

APPROX. RE.	67,500	54,000	26,000	14,000	6,700
P_1-P_2(in.H_2O)	31.16	22.40	5.66	1.47	0.38
P_1-P_3(in.H_2O)	28.75	20.63	5.29	1.43	0.48
P_2-P_0(in.Hg.)	5.71	3.90	0.89	0.24	0.12
P_3-P_0(in.H_2O)	- -	- -	- -	- -	- -
T_0(Deg.)	85.60	85.00	84.60	84.60	84.40
T_A(MV.)	1.549	1.550	1.551	1.556	1.557
T_W(MV.)	5.372	5.372	5.370	5.370	5.371
BI_1	5.114	5.134	5.210	5.261	5.295
BI_2	5.097	5.125	5.203	5.258	5.294
BI_3	5.028	5.049	5.153	5.224	5.263
BI_4	4.934	4.971	5.085	5.172	5.221
BI_5	4.880	4.920	5.041	5.130	5.206
BI_6	4.984	5.016	5.094	5.157	5.205
I_1	0.417	0.378	0.241	0.159	0.108
I_2	0.508	0.461	0.303	0.199	0.126
I_3	0.598	0.540	0.361	0.237	0.153
I_4	0.515	0.460	0.298	0.193	0.123
I_5	0.552	0.496	0.325	0.208	0.128
I_6	0.546	0.492	0.322	0.202	0.133
I_7	0.759	0.694	0.478	0.312	0.223
I_8	0.716	0.658	0.448	0.292	0.210
I_9	0.788	0.720	0.490	0.313	0.239
I_{10}	1.016	0.944	0.691	0.488	0.370
I_{11}	1.049	0.978	0.717	0.515	0.382
I_{12}	1.203	1.117	0.848	0.662	0.445
I_{13}	1.261	1.168	0.873	0.676	0.459
I_{14}	1.138	1.076	0.865	0.697	0.553

Note: All "BI" and "I" values in millivolts.

Nozzle Diameter - 0.250 in.
Vertical Setting, Z_n - 1.00 in.
Approximate Z_n/D - 4
Barometric Pressure - 30.414 in. Hg.

APPROX. RE.	67,500	54,000	26,000	14,000	6,700
P_1-P_2(in.H_2O)	30.86	22.49	5.57	1.33	0.30
P_1-P_3(in.H_2O)	28.43	20.74	5.18	1.32	0.39
P_2-P_0(in.Hg.)	5.66	3.90	0.92	0.29	0.15
P_3-P_0(in.H_2O)	- -	- -	- -	- -	- -
T_0(Deg.)	84.60	84.80	84.40	84.50	84.80
T_A(MV.)	1.523	1.526	1.537	1.547	1.566
T_W(MV.)	5.363	5.362	5.364	5.363	5.362
BI_1	5.113	5.138	5.212	5.261	5.291
BI_2	5.089	5.113	5.194	5.254	5.288
BI_3	5.004	5.036	5.144	5.219	5.265
BI_4	4.938	4.969	5.097	5.176	5.232
BI_5	4.892	4.928	5.061	5.150	5.198
BI_6	5.037	5.049	5.136	5.185	5.222
I_1	0.467	0.428	0.274	0.177	0.115
I_2	0.550	0.502	0.329	0.213	0.139
I_3	0.672	0.622	0.420	0.284	0.192
I_4	0.567	0.518	0.329	0.203	0.124
I_5	0.602	0.553	0.358	0.216	0.132
I_6	0.587	0.536	0.348	0.223	0.141
I_7	0.810	0.741	0.500	0.323	0.203
I_8	0.752	0.694	0.467	0.303	0.139
I_9	0.835	0.763	0.517	0.333	0.214
I_{10}	1.009	0.937	0.674	0.466	0.326
I_{11}	1.061	0.972	0.702	0.488	0.339
I_{12}	1.137	1.057	0.794	0.592	0.475
I_{13}	1.186	1.116	0.830	0.613	0.474
I_{14}	1.192	1.120	0.913	0.742	0.592

Note: All "BI" and "I" values in millivolts.

Nozzle Diameter - 0.250 in.
Vertical Setting, Z_n - 1.75 in.
Approximate Z_n/D - 7
Barometric Pressure - 30.446 in. Hg.

APPROX. RE.	67,500	54,000	26,000	14,000	6,700
P_1-P_2(in.H_2O)	31.44	22.52	5.53	1.38	0.38
P_1-P_3(in.H_2O)	29.00	20.80	5.00	1.15	0.52
P_2-P_0(in.Hg.)	5.72	3.93	0.90	0.30	0.15
P_3-P_0(in.H_2O)	- -	- -	- -	- -	- -
T_0(Deg.)	84.70	84.40	84.60	84.40	84.50
T_A(MV.)	1.550	1.543	1.545	1.549	1.558
T_W(MV.)	5.370	5.372	5.373	5.373	5.373
BI_1	5.107	5.132	5.210	5.263	5.290
BI_2	5.089	5.112	5.200	5.256	5.288
BI_3	5.012	5.043	5.153	5.226	5.264
BI_4	4.947	4.989	5.106	5.192	5.238
BI_5	4.922	4.963	5.080	5.168	5.216
BI_6	4.974	5.001	5.090	5.164	5.206
I_1	0.520	0.381	0.248	0.170	0.122
I_2	0.526	0.476	0.309	0.207	0.147
I_3	0.543	0.497	0.339	0.229	0.162
I_4	0.524	0.475	0.306	0.201	0.140
I_5	0.563	0.509	0.331	0.218	0.148
I_6	0.547	0.501	0.330	0.216	0.144
I_7	0.777	0.714	0.478	0.318	0.227
I_8	0.728	0.662	0.448	0.301	0.211
I_9	0.800	0.737	0.500	0.331	0.232
I_{10}	0.963	0.894	0.633	0.425	0.313
I_{11}	0.993	0.925	0.663	0.451	0.335
I_{12}	1.098	1.048	0.776	0.554	0.429
I_{13}	1.137	1.077	0.787	0.567	0.435
I_{14}	1.146	1.089	0.874	0.678	0.559

Note: All "BI" and "I" values in millivolts.

Nozzle Diameter - 0.250 in.
Vertical Setting, Z_n - 3.50 in.
Approximate Z_n/D - 14
Barometric Pressure - 30.446 in. Hg.

APPROX. RE.	67,500	54,000	26,000	14,000	6,700
P_1-P_2(in.H_2O)	31.08	22.61	5.64	1.50	0.35
P_1-P_3(in.H_2O)	28.71	20.90	5.22	1.47	0.50
P_2-P_0(in.Hg.)	5.68	3.95	0.95	0.31	0.15
P_3-P_0(in.H_2O)	- -	- -	- -	- -	- -
T_0(Deg.)	84.80	84.80	84.20	84.20	84.40
T_A(MV.)	1.550	1.550	1.558	1.566	1.568
T_W(MV.)	5.376	5.374	5.377	5.377	5.376
BI_1	5.112	5.143	5.215	5.264	5.297
BI_2	5.099	5.125	5.202	5.260	5.295
BI_3	5.038	5.072	5.168	5.241	5.277
BI_4	5.014	5.043	5.140	5.222	5.263
BI_5	4.988	5.018	5.118	5.204	5.244
BI_6	5.020	5.052	5.128	5.206	5.243
I_1	0.448	0.410	0.273	0.189	0.131
I_2	0.527	0.475	0.376	0.224	0.148
I_3	0.550	0.509	0.358	0.252	0.172
I_4	0.530	0.479	0.324	0.216	0.145
I_5	0.550	0.500	0.338	0.223	0.145
I_6	0.536	0.503	0.342	0.226	0.147
I_7	0.713	0.652	0.451	0.286	0.195
I_8	0.668	0.612	0.425	0.277	0.189
I_9	0.727	0.672	0.466	0.297	0.204
I_{10}	0.831	0.762	0.538	0.354	0.262
I_{11}	0.853	0.787	0.568	0.373	0.268
I_{12}	0.910	0.843	0.624	0.445	0.340
I_{13}	0.952	0.887	0.654	0.465	0.342
I_{14}	1.003	0.948	0.748	0.539	0.421

Note: All "BI" and "I" values in millivolts.

Nozzle Diameter - 0.250 in.
Vertical Setting, Z_n - 5.00 in.
Approximate Z_n/D - 20
Barometric Pressure - 30.446 in. Hg.

APPROX. RE.	67,500	54,000	26,000	14,000	6,700
P_1-P_2(in.H_2O)	31.44	22.48	5.56	1.43	0.31
P_1-P_3(in.H_2O)	29.02	21.76	5.15	1.36	0.37
P_2-P_0(in.Hg.)	5.73	3.90	0.90	0.23	0.10
P_3-P_0(in.H_2O)	- -	- -	- -	- -	- -
T_0(Deg.)	84.60	84.40	83.60	73.00	82.80
T_A(MV.)	1.554	1.548	1.545	1.53	1.51
T_W(MV.)	5.378	5.380	5.380	5.370	5.370
BI_1	5.126	5.148	5.225	5.262	5.297
BI_2	5.115	5.136	5.218	5.262	5.296
BI_3	5.078	5.103	5.193	5.248	5.283
BI_4	5.057	5.083	5.179	5.232	5.269
BI_5	5.037	5.062	5.150	5.212	5.253
BI_6	5.068	5.087	5.163	5.223	5.261
I_1	0.460	0.416	0.279	0.192	0.130
I_2	0.544	0.492	0.329	0.223	0.142
I_3	0.577	0.522	0.359	0.249	0.163
I_4	0.522	0.470	0.310	0.205	0.133
I_5	0.543	0.488	0.326	0.215	0.133
I_6	0.528	0.481	0.324	0.213	0.136
I_7	0.647	0.586	0.397	0.262	0.175
I_8	0.609	0.548	0.379	0.250	0.163
I_9	0.656	0.596	0.410	0.265	0.177
I_{10}	0.741	0.676	0.473	0.320	0.237
I_{11}	0.764	0.703	0.498	0.332	0.235
I_{12}	0.810	0.761	0.576	0.408	0.324
I_{13}	0.866	0.808	0.615	0.434	0.335
I_{14}	0.924	0.863	0.673	0.468	0.374

Note: All "BI" and "I" values in millivolts.

Nozzle Diameter - 0.250 in.
Vertical Setting, Z_n - 7.50 in.
Approximate Z_n/D - 30
Barometric Pressure - 30.475 in. Hg.

APPROX. RE.	67,500	54,000	26,000	14,000	6,700
P_1-P_2(in.H_2O)	31.04	23.00	5.53	1.44	0.32
P_1-P_3(in.H_2O)	28.65	21.22	5.08	1.45	0.43
P_2-P_0(in.Hg.)	5.67	3.99	0.91	0.30	0.10
P_3-P_0(in.H_2O)	- -	- -	- -	- -	- -
T_0(Deg.)	82.0	81.5	82.2	82.4	82.6
T_A(MV.)	1.473	1.459	1.473	1.488	1.481
T_W(MV.)	5.383	5.372	5.383	1.383	5.383
BI_1	5.152	5.176	5.237	5.282	5.310
BI_2	5.148	5.168	5.239	5.286	5.312
BI_3	5.125	5.148	5.224	5.274	5.303
BI_4	5.112	5.133	5.209	5.262	5.283
BI_5	5.093	5.111	5.196	5.253	5.284
BI_6	5.154	5.185	5.229	5.278	5.303
I_1	0.457	0.415	0.273	0.189	0.128
I_2	0.503	0.459	0.322	0.221	0.154
I_3	0.579	0.525	0.334	0.230	0.161
I_4	0.463	0.427	0.274	0.182	0.127
I_5	0.485	0.447	0.290	0.189	0.128
I_6	0.480	0.442	0.281	0.182	0.122
I_7	0.562	0.517	0.341	0.236	0.168
I_8	0.530	0.493	0.323	0.215	0.150
I_9	0.571	0.523	0.348	0.224	0.148
I_{10}	0.628	0.581	0.398	0.279	0.206
I_{11}	0.648	0.609	0.420	0.282	0.201
I_{12}	0.686	0.650	0.457	0.333	0.253
I_{13}	0.743	0.706	0.509	0.357	0.258
I_{14}	0.799	0.749	0.571	0.410	0.301

Note: All "BI" and "I" values in millivolts.

Nozzle Diameter - 0.250 in.
Vertical Setting, Z_n - 9.94 in.
Approximate Z_n/D - 40
Barometric Pressure - 30.362 in. Hg.

APPROX. RE.	67,500	54,000	26,000	14,000	6,700
P_1-P_2(in.H_2O)	31.85	22.55	5.58	1.47	0.33
P_1-P_3(in.H_2O)	29.34	20.68	5.05	1.35	0.30
P_2-P_0(in.Hg.)	5.90	3.95	0.86	0.25	0.1
P_3-P_0(in.H_2O)	- -	- -	- -	- -	- -
T_0(Deg.)	87.0	86.0	86.0	86.0	86.0
T_A(MV.)	1.589	1.589	1.598	1.603	1.603
T_W(MV.)	5.380	5.378	5.376	5.371	5.370
BI_1	5.188	5.208	5.262	5.294	5.318
BI_2	5.185	5.200	5.259	5.296	5.318
BI_3	5.164	5.180	5.242	5.284	5.311
BI_4	5.152	51.72	5.232	5.282	5.301
BI_5	5.149	5.159	5.219	5.271	5.296
BI_6	5.189	5.202	5.251	5.289	5.310
I_1	0.376	0.337	0.219	0.152	0.111
I_2	0.390	0.344	0.233	0.154	0.114
I_3	0.473	0.419	0.279	0.185	0.126
I_4	0.391	0.349	0.224	0.155	0.110
I_5	0.387	0.342	0.228	0.193	0.100
I_6	0.403	0.358	0.236	0.152	0.105
I_7	0.464	0.414	0.281	0.195	0.142
I_8	0.449	0.400	0.273	0.173	0.147
I_9	0.465	0.418	0.280	0.177	0.125
I_{10}	0.522	0.470	0.331	0.232	0.169
I_{11}	0.536	0.487	0.346	0.180	0.152
I_{12}	0.549	0.498	0.354	0.242	0.177
I_{13}	0.585	0.530	0.383	0.238	0.177
I_{14}	0.621	0.570	0.417	0.278	0.202

Note: All "BI" and "I" values in millivolts.

Nozzle Diameter - 0.250 in.
Vertical Setting, Z_n - 12.31 in.
Approximate Z_n/D - 50
Barometric Pressure - 30.362 in. Hg.

APPROX. RE.	67,500	54,000	26,000	14,000	6,700
P_1-P_2(in.H_2O)	30.80	22.35	5.56	1.65	0.35
P_1-P_3(in.H_2O)	28.20	20.40	5.05	1.48	0.3
P_2-P_0(in.Hg.)	5.57	3.83	0.9	0.3	0.1
P_3-P_0(in.H_2O)	- -	- -	- -	- -	- -
T_0(Deg.)	85.5	86.0	86.0	8600	86.0
T_A(MV.)	1.554	1.558	1.577	1.596	1.599
T_W(MV.)	5.371	5.377	5.384	5.387	5.388
BI_1	5.214	5.231	5.278	5.306	5.327
BI_2	5.208	5.223	5.273	5.303	5.327
BI_3	5.187	5.205	5.259	5.294	5.319
BI_4	5.185	5.199	5.255	5.291	5.319
BI_5	5.172	5.187	5.243	5.284	5.313
BI_6	5.215	5.231	5.273	5.303	5.323
I_1	0.348	0.317	0.213	0.154	0.111
I_2	0.354	0.317	0.214	0.147	0.101
I_3	0.406	0.360	0.237	0.164	0.112
I_4	0.359	0.323	0.211	0.153	0.106
I_5	0.365	0.313	0.199	0.133	0.081
I_6	0.365	0.324	0.218	0.145	0.094
I_7	0.425	0.388	0.267	0.190	0.133
I_8	0.402	0.372	0.252	0.173	0.100
I_9	0.428	0.389	0.264	0.175	0.111
I_{10}	0.476	0.437	0.308	0.214	0.145
I_{11}	0.469	0.433	0.305	0.197	0.125
I_{12}	0.480	0.447	0.315	0.215	0.142
I_{13}	0.506	0.473	0.338	0.218	0.142
I_{14}	0.526	0.491	0.353	0.240	0.163

Note: All "BI" and "I" values in millivolts.

Nozzle Diameter - 0.375 in.
Vertical Setting, Z_n - 0.375 in.
Approximate Z_n/D - 1
Barometric Pressure - 30.162 in. Hg.

APPROX. RE.	67,500	54,000	26,000	14,000	6,700
P_1-P_2(in.H_2O)	5.88(in.Hg)	4.01(in.Hg)	15.98	4.01	0.92
P_1-P_3(in.H_2O)	- -	- -	14.52	3.58	0.78
P_2-P_0(in.Hg.)	2.25	0.96	0.34	0.1	0.05
P_3-P_0(in.H_2O)	37.37	24.86	- -	- -	- -
T_0(Deg.)	88.0	87.80	87.50	87.50	87.40
T_A(MV.)	1.618	1.619	1.627	1.634	1.632
T_W(MV.)	5.361	5.362	5.360	5.360	5.360
BI_1	5.117	5.165	5.215	5.260	5.296
BI_2	5.093	5.128	5.198	5.251	5.290
BI_3	4.903	4.952	5.076	5.169	5.238
BI_4	4.939	4.989	5.088	5.168	5.238
BI_5	5.049	5.091	5.163	5.212	5.255
BI_6	5.081	5.113	5.173	5.214	5.247
I_1	0.401	0.373	0.258	0.164	0.094
I_2	0.422	0.388	0.271	0.174	0.102
I_3	0.424	0.390	0.274	0.175	0.102
I_4	0.543	0.488	0.340	0.214	0.120
I_5	0.552	0.499	0.346	0.218	0.124
I_6	0.572	0.521	0.363	0.227	0.130
I_7	0.800	0.725	0.523	0.341	0.206
I_8	0.756	0.683	0.500	0.331	0.198
I_9	0.806	0.732	0.538	0.351	0.211
I_{10}	0.946	0.861	0.646	0.466	0.288
I_{11}	0.987	0.906	0.687	0.496	0.313
I_{12}	0.863	0.792	0.634	0.497	0.342
I_{13}	0.898	0.831	0.676	0.527	0.363
I_{14}	0.861	0.819	0.681	0.539	0.398

Note: All "BI" and "I" values in millivolts.

Nozzle Diameter - 0.375 in.
Vertical Setting, Z_n - 1.50 in.
Approximate Z_n/D - 4
Barometric Pressure - 30.162 in. Hg.

APPROX. RE.	67,500	54,000	26,000	14,000	6,700
P_1-P_2(in.H_2O)	5.98(in.Hg.)	4.00(in.Hg)	15.84	4.07	0.94
P_1-P_3(in.H_2O)	- -	- -	14.41	3.68	0.80
P_2-P_0(in.Hg.)	2.27	1.43	0.34	0.1	0.06
P_3-P_0(in.H_2O)	37.62	24.34	- -	- -	- -
T_0(Deg.)	87.20	87.50	87.60	87.40	87.40
T_A(MV.)	1.599	1.599	1.607	1.617	1.626
T_W(MV.)	5.360	5.360	5.360	5.362	5.362
BI_1	5.133	5.154	5.216	5.264	5.297
BI_2	5.102	5.130	5.198	5.252	5.240
BI_3	4.915	4.964	5.082	5.175	5.243
BI_4	4.979	5.018	5.112	5.192	5.244
BI_5	5.087	5.099	5.168	5.218	5.259
BI_6	5.106	5.115	51175	5.217	5.253
I_1	0.437	0.392	0.262	0.172	0.105
I_2	0.452	0/400	0.274	0.183	0.113
I_3	0.455	0.405	0.274	0.181	0.113
I_4	0.569	0.502	0.340	0.219	0.130
I_5	0.596	0.528	0.354	0.235	0.139
I_6	0.605	0.544	0.368	0.241	0.140
I_7	0.792	0.713	0.504	0.332	0.203
I_8	0.772	0.696	0.497	0.336	0.207
I_9	0.822	0.736	0.526	0.346	0.209
I_{10}	0.895	0.815	0.597	0.418	0.288
I_{11}	0.943	0.863	0.567	0.444	0.313
I_{12}	0.913	0.828	0.633	0.478	0.347
I_{13}	0.928	0.851	0.663	0.517	0.374
I_{14}	0.910	0.852	0.707	0.562	0.417

Note: All "BI" and "I" values in millivolts.

Nozzle Diameter - 0.375 in.
Vertical Setting, Z_n - 2.625 in.
Approximate Z_n/D - 7
Barometric Pressure - 30.162 in. Hg.

APPROX. RE.	67,500	54,000	26,000	14,000	6,700
P_1-P_2(in.H_2O)	5.96(in.Hg.)	4.03(in.Hg)	15.93	4.00	1.00
P_1-P_3(in.H_2O)	- -	- -	14.47	3.64	0.85
P_2-P_0(in.Hg.)	2.26	1.45	0.39	0.12	0.06
P_3-P_0(in.H_2O)	37.60	24.65	- -	- -	- -
T_0(Deg.)	87.40	86.80	85.70	86.00	86.40
T_A(MV.)	1.600	1.601	1.593	1.599	1.609
T_W(MV.)	5.359	5.360	5.360	5.361	5.364
BI_1	5.126	5.151	5.221	5.269	5.299
BI_2	5.097	5.124	5.201	5.258	5.292
BI_3	4.929	4.969	5.092	5.189	5.250
BI_4	4.995	5.031	5.151	5.217	5.258
BI_5	5.055	5.082	5.164	5.222	5.260
BI_6	5.082	5.111	5.166	5.222	5.263
I_1	0.446	0.398	0.266	0.176	0.114
I_2	0.443	0.398	0.284	0.190	0.123
I_3	0.448	0.398	0.281	0.186	0.120
I_4	0.564	0.504	0.339	0.216	0.132
I_5	0.578	0.520	0.369	0.239	0.148
I_6	0.584	0.517	0.360	0.232	0.143
I_7	0.760	0.685	0.473	0.303	0.187
I_8	0.736	0.665	0.488	0.320	0.204
I_9	0.773	0.698	0.492	0.315	0.194
I_{10}	0.836	0.759	0.557	0.371	0.245
I_{11}	0.887	0.813	0.604	0.405	0.278
I_{12}	0.896	0.833	0.642	0.453	0.317
I_{13}	0.945	0.878	0.688	0.503	0.357
I_{14}	0.987	0.948	0.764	0.580	0.419

Note: All "BI" and "I" values in millivolts.

Nozzle Diameter - 0.375 in.
Vertical Setting, Z_n - 5.25 in.
Approximate Z_n/D - 14
Barometric Pressure - 30.203 in. Hg.

APPROX. RE.	67,500	54,000	26,000	14,000	6,700
P_1-P_2(in.H_2O)	5.90(in.Hg.)	4.01(In.Hg)	15.97	3.93	0.94
P_1-P_3(in.H_2O)	- -	- -	14.54	3.49	0.86
P_2-P_0(in.Hg.)	2.26	1.46	0.35	0.10	0.05
P_3-P_0(in.H_2O)	37.15	24.73	- -	- -	- -
T_0(Deg.)	86.90	86.60	86.10	86.10	86.20
T_A(MV.)	1.612	1.601	1.575	1.578	1.592
T_W(MV.)	5.353	5.353	5.354	5.355	5.353
BI_1	5.137	5.160	5.221	5.267	5.295
BI_2	5.121	5.144	5.201	5.258	5.290
BI_3	4.993	5.032	5.130	5.210	5.259
BI_4	5.054	5.085	5.163	5.228	5.269
BI_5	5.033	5.062	5.140	5.213	5.262
BI_6	5.087	5.110	5.172	5.233	5.272
I_1	0.458	0.409	0.287	0.189	0.126
I_2	0.438	0.391	0.276	0.183	0.122
I_3	0.464	0.413	0.297	0.196	0.129
I_4	0.542	0.485	0.333	0.210	0.133
I_5	0.572	0.516	0.370	0.240	0.153
I_6	0.572	0.510	0.359	0.232	0.148
I_7	0.636	0.566	0.404	0.260	0.165
I_8	0.647	0.584	0.430	0.282	0.180
I_9	0.672	0.603	0.428	0.278	0.178
I_{10}	0.699	0.630	0.458	0.308	0.203
I_{11}	0.757	0.681	0.499	0.337	0.223
I_{12}	0.752	0.697	0.525	0.359	0.233
I_{13}	0.807	0.742	0.567	0.388	0.261
I_{14}	0.842	0.786	0.613	0.413	0.279

Note: All "BI" and "I" values in millivolts.

Nozzle Diameter - 0.375 in.
Vertical Setting, Z_n - 7.50 in.
Approximate Z_n/D - 20
Barometric Pressure - 30.203 in. Hg.

APPROX. RE.	67,500	54,000	26,000	14,000	6,700
P_1-P_2(in.H_2O)	5.95(in.Hg.)	3.99(in.Hg)	16.00	4.06	0.94
P_1-P_3(in.H_2O)	- -	- -	14.56	3.63	0.87
P_2-P_0(in.Hg.)	2.30	1.45	0.38	0.10	0.08
P_3-P_0(in.H_2O)	38.03	24.37	- -	- -	- -
T_0(Deg.)	87.60	87.60	87.40	87.20	86.80
T_A(MV.)	1.612	1.605	1.600	1.593	1.597
T_W(MV.)	5.343	5.343	5.343	5.341	5.353
BI_1	5.144	5.168	5.220	5.266	5.299
BI_2	5.136	5.161	5.218	5.262	5.297
BI_3	5.039	5.075	5.153	5.219	5.270
BI_4	5.091	5.123	5.179	5.233	5.282
BI_5	5.074	5.103	5.163	5.219	5.276
BI_6	5.118	5.140	5.197	5.242	5.288
I_1	0.433	0.390	0.272	0.182	0.121
I_2	0.423	0.378	0.263	0.178	0.116
I_3	0.441	0.398	0.275	0.181	0.118
I_4	0.476	0.428	0.292	0.192	0.121
I_5	0.524	0.469	0.316	0.208	0.137
I_6	0.503	0.453	0.306	0.199	0.124
I_7	0.554	0.502	0.342	0.232	0.154
I_8	0.571	0.521	0.357	0.241	0.164
I_9	0.576	0.519	0.353	0.237	0.147
I_{10}	0.596	0.557	0.397	0.281	0.188
I_{11}	0.634	0.587	0.422	0.299	0.194
I_{12}	0.640	0.588	0.441	0.307	0.192
I_{13}	0.676	0.624	0.469	0.326	0.202
I_{14}	0.679	0.643	0.499	0.343	0.221

Note: All "BI" and "I" values in millivolts.

Nozzle Diameter - 0.375 in.
Vertical Setting, Z_n - 11.25 in.
Approximate Z_n/D - 30
Barometric Pressure - 30.203 in. Hg.

APPROX. RE.	67,500	54,000	26,000	14,000	6,700
P_1-P_2(in.H_2O)	5.95(in.Hg)	4.02(In.Hg)	16.04	4.04	0.93
P_1-P_3(in.H_2O)	- -	- -	14.60	3.64	0.86
P_2-P_0(in.Hg.)	2.28	1.47	0.40	0.11	0.06
P_3-P_0(in.H_2O)	37.88	24.82	- -	- -	- -
T_0(Deg.)	87.40	87.60	87.60	87.40	87.20
T_A(MV.)	1.615	1.614	1.624	1.628	1.626
T_W(MV.)	5.350	5.352	5.358	5.360	5.352
BI_1	5.184	5.206	5.256	5.291	5.304
BI_2	5.182	5.205	5.251	5.287	5.302
BI_3	5.106	5.138	5.203	5.256	5.282
BI_4	5.153	5.171	5.229	5.271	5.295
BI_5	5.139	5.163	5.220	5.269	5.294
BI_6	5.179	5.198	5.246	5.284	5.302
I_1	0.365	0.329	0.232	0.160	0.111
I_2	0.355	0.319	0.228	0.152	0.106
I_3	0.373	0.331	0.238	0.161	0.109
I_4	0.388	0.342	0.243	0.168	0.115
I_5	0.417	0.369	0.272	0.173	0.112
I_6	0.401	0.359	0.256	0.168	0.110
I_7	0.440	0.392	0.292	0.200	0.135
I_8	0.457	0.404	0.305	0.201	0.132
I_9	0.467	0.413	0.300	0.200	0.122
I_{10}	0.469	0.423	0.324	0.223	0.140
I_{11}	0.507	0.454	0.344	0.226	0.123
I_{12}	0.498	0.456	0.347	0.236	0.146
I_{13}	0.533	0.487	0.367	0.243	0.145
I_{14}	0.530	0.487	0.368	0.248	0.152

Note: All "BI" and "I" values in millivolts.

Nozzle Diameter - 0.375 in.
Vertical Setting, Z_n - 15.00 in.
Approximate Z_n/D - 40
Barometric Pressure - 30.203 in. Hg.

APPROX. RE.	67,500	54,000	26,000	14,000	6,700
P_1-P_2(in.H_2O)	5.88(in.Hg.)	4.00(in.Hg)	16.27	4.00	0.93
P_1-P_3(in.H_2O)	- -	- -	14.80	3.58	0.87
P_2-P_0(in.Hg.)	2.20	1.47	0.36	0.10	0.07
P_3-P_0(in.H_2O)	36.77	24.40	- -	- -	- -
T_0(Deg.)	86.00	86.20	86.60	86.80	86.90
T_A(MV.)	1.585	1.586	1.594	1.607	1.614
T_W(MV.)	5.358	5.361	5.361	5.362	5.362
BI_1	5.212	5.230	5.269	5.297	5.317
BI_2	5.214	5.231	5.268	5.298	5.318
BI_3	5.151	5.175	5.232	5.272	5.304
BI_4	5.191	5.208	5.261	5.288	5.313
BI_5	5.185	5.203	5.249	5.283	5.310
BI_6	5.230	5.243	5.272	5.301	5.320
I_1	0.333	0.292	0.209	0.147	0.112
I_2	0.319	0.276	0.200	0.129	0.088
I_3	0.345	0.300	0.213	0.140	0.095
I_4	0.340	0.302	0.215	0.143	0.104
I_5	0.354	0.308	0.221	0.139	0.091
I_6	0.357	0.317	0.220	0.145	0.095
I_7	0.371	0.333	0.240	0.167	0.106
I_8	0.368	0.329	0.236	0.154	0.102
I_9	0.389	0.350	0.217	0.163	0.100
I_{10}	0.395	0.358	0.263	0.178	0.113
I_{11}	0.384	0.386	0.244	0.180	0.104
I_{12}	0.411	0.373	0.271	0.176	0.115
I_{13}	0.439	0.400	0.282	0.182	0.113
I_{14}	0.470	0.412	0.302	0.189	0.136

Note: All "BI" and "I" values in millivolts.

REFERENCES

1. Abramovich, G.N., "The Theory of Turbulent Jets," The M.I.T. Press, Massachusetts Institute of Technology, Cambridge, Massachusetts, 1963.

2. Bluston, H.S., "An Experimental Study of Jet Turbulent Mixing at Subsonic - Supersonic Speeds", AIAA Journal, Vol 4, 1966, pp. 1137-1139.

3. Gardon, R., Akfirat, J.C., "Heat Transfer Characteristics of Impinging Two-Dimensional Air Jets", Journal of Heat Transfer, Trans. ASME, Series C, Vol. 88, 1966, pp. 101-108.

4. Gardon, R. and Cobonpue, J., "Heat Transfer Between a Flat Plate and Jets of Air Impinging on It", International Developments in Heat Transfer, Proceedings 2nd International Heat Transfer Conference, ASME, New York, N. Y., 1962, pp. 454-460.

5. Huang, G.C., "Investigations of Heat Transfer Coefficients for Air Flow Through Round Jets Impinging Normal to a Heat Transfer Surface", Journal of Heat Transfer, Trans. ASME, Series C, Vol. 85, 1963, pp. 237-243.

6. Pai, S., "Fluid Dynamics of Jets", D. Van Nostrand Company, Inc., New York, N. Y., 1954.

7. Perry, K.P., "Heat Transfer by Convection From a Hot Gas Jet to a Plane Surface", Proceedings, The Institute of Mechanical Engineers, London, England, Vol. 168, 1965, pp. 775-780.

8. Schlichting, H., "Boundary Layer Theory", McGraw-Hill Book Company, Inc., New York, N.Y., 1960, Second Edition.

9. Smirnov, V.A., Verevochkin, G.E., and Brdlick, P.M., "Heat Transfer Between a Jet and a Held Plate Normal to Flow", International Journal of Heat and Mass Transfer, Vol 2, 1961, pp. 1-7.

10. Supplement to ASME Power Test Codes, Chapter 4, Flow Measurement, The American Society of Mechanical Engineers, New York, N.Y., 1959.

11. Vickers, J.M.F., "Heat Transfer Coefficients Between Fluid Jets and Normal Surfaces", Industrial and Engineering Chemistry, Vol. 51, 1959, pp. 967-972.